

JGR Atmospheres



RESEARCH ARTICLE

10.1029/2025JD043923

Special Collection:

TEMPO Data Products, Science, and Applications

Key Points:

- Tropospheric Emissions: Monitoring of Pollution (TEMPO) data correlate to surface NO₂ moderately (R² = 0.42) and correlation improves at longer timescales at monitors not near roads (R² = 0.61)
- TEMPO slant columns (R² = 0.72) outperform TROPOMI (R² = 0.65) and TEMPO (R² = 0.66) vertical columns due to uncertainty from the air mass factor
- TEMPO vertical columns perform worse relative to monitors in the early morning when TEMPO is less sensitive to near-surface pollution

Supporting Information:

Supporting Information may be found in the online version of this article.

Correspondence to:

M. O. Nawaz, nawazm3@cardiff.ac.uk

Citation:

Nawaz, M. O., Huber, D. E., Kerr, G. H., Judd, L. M., Acker, S. J., & Goldberg, D. L. (2025). A comparative analysis of TEMPO NO₂ remote sensing with surface-level monitoring through diurnal and seasonal trends, meteorology, and monitor characteristics. *Journal of Geophysical Research: Atmospheres, 130*, e2025JD043923. https://doi.org/10.1029/2025JD043923

Received 24 MAR 2025 Accepted 9 OCT 2025

Author Contributions:

Conceptualization: M. Omar Nawaz, Daniel L. Goldberg Data curation: M. Omar Nawaz, Daniel E. Huber, Summer J. Acker, Daniel L. Goldberg

© 2025. The Author(s).

This is an open access article under the terms of the Creative Commons

Attribution License, which permits use, distribution and reproduction in any medium, provided the original work is properly cited.

A Comparative Analysis of TEMPO NO₂ Remote Sensing With Surface-Level Monitoring Through Diurnal and Seasonal Trends, Meteorology, and Monitor Characteristics

M. Omar Nawaz^{1,2}, Daniel E. Huber¹, Gaige H. Kerr¹, Laura M. Judd³, Summer J. Acker⁴, and Daniel L. Goldberg¹

¹Department of Environmental and Occupational Health, George Washington University, Washington, DC, USA, ²School of Earth and Environmental Sciences, Cardiff University, Cardiff, UK, ³Langley Research Center, National Aeronautics and Space Administration, Hampton, VA, USA, ⁴Nelson Institute Center for Sustainability and the Global Environment, University of Wisconsin-Madison, Madison, WI, USA

Abstract The NASA Tropospheric Emissions: Monitoring of Pollution (TEMPO) instrument—launched in August 2023—measures diurnal patterns of column NO2 at unprecedented spatial resolution. Given its nascent status, it is unknown how TEMPO V03 column NO2 compares to surface-level monitoring across long-term timescales. In this study, we explore how temporally averaged hourly TEMPO column NO₂ observations compare to surface-level concentrations from monitors in the US EPA Air Quality System (AQS). Monthly averaged hourly TEMPO vertical column densities (VCDs) correlate to surface-level NO2 moderately $(R^2 = 0.42)$; however, there is notably stronger correlation for monitors that are not defined as "near road" across hourly annual-average equivalent timescales ($R^2 = 0.61$). During the TROPOMI overpass (approximately 13:30 LT), annual-average TEMPO slant column densities (SCDs) at "not near road" sites are better correlated with surface-level NO₂ ($R^2 = 0.72$) than tropospheric VCDs from TROPOMI ($R^2 = 0.65$) and TEMPO ($R^2 = 0.66$) due to added uncertainty with a priori inputs in the AMF. In the future, a more accurate AMF could improve TEMPO VCDs correlation to the level of the TEMPO SCDs. TEMPO column NO2 are most poorly correlated in the early morning at 6:00 ($R^2 = 0.23$) and 7:00 ($R^2 = 0.35$) LT when TEMPO is less sensitive to near-surface pollution due to a longer sunlight path through the atmosphere and the subsequent increased sensitivity to retrieval assumptions. Ultimately, this analysis identifies conditions and characteristics that affect the correlation between TEMPO and ground-level monitoring that has implications for applying TEMPO remote sensing data to derive or interpret surface-level NO₂.

Plain Language Summary The NASA Tropospheric Emissions: Monitoring of Pollution (TEMPO) satellite instrument measures hourly levels of NO₂—a pollutant that is associated with fossil fuel burning—at great spatial detail. Given that TEMPO was recently launched, it is not clear how well it compares to NO₂ monitors on the ground. In this study, we compare satellite measurements of NO₂ from TEMPO with monitors from the US EPA. We find that there is generally good agreement between the two, especially when comparing across longer timeframes and for monitors that are not directly near major highways. We also consider how different weather conditions could influence the comparison and find that the boundary layer height influences this relationship. Ultimately, we identify some of the characteristics that influence the relationship between satellite and ground level measurement of NO₂ that have implications for future modeling and health studies.

1. Introduction

Nitrogen dioxide (NO_2) is a trace gas that is a byproduct of both anthropogenic activities and natural processes (Zhang et al., 2003). The extreme temperatures reached in fossil fuel combustion, atmospheric lightning, and wildfires present a conducive environment for fuel-bound or ambient nitrogen (N_2) to spontaneously react with oxygen (O_2) to form NO_2 (Jacob et al., 1996); microbial activity is also responsible for its emission (Lerdau et al., 2000). Given its adverse effects on health, NO_2 is classified as an air pollutant by the World Health Organization (WHO, 2025) and the United States (US) Environmental Protection Agency (EPA) (US EPA, 2014). Exposure to NO_2 is associated with pediatric asthma (Achakulwisut et al., 2019; Anenberg et al., 2022; Khreis et al., 2017) and premature death (Chen et al., 2024). A key feature of NO_2 is its short atmospheric lifetime that generally varies between 2 and 8 hr during the daytime (Laughner & Cohen, 2019) and is dependent on seasonally varying meteorology, ozone titration, and emission patterns. Owing to this relatively rapid removal from the

NAWAZ ET AL. 1 of 22



Formal analysis: M. Omar Nawaz, Daniel L. Goldberg

Funding acquisition: Daniel L. Goldberg Investigation: M. Omar Nawaz Methodology: M. Omar Nawaz, Gaige H. Kerr, Laura M. Judd, Daniel

Project administration: Daniel

L. Goldberg **Project admi**L. Goldberg

Resources: Daniel E. Huber, Gaige H. Kerr, Summer J. Acker, Daniel

L. Goldberg

Software: M. Omar Nawaz Supervision: Daniel L. Goldberg Validation: M. Omar Nawaz, Gaige H. Kerr, Laura M. Judd, Daniel L. Goldberg

Visualization: M. Omar Nawaz, Daniel L. Goldberg

Writing – original draft: M. Omar Nawaz Writing – review & editing:

M. Omar Nawaz, Daniel E. Huber, Gaige H. Kerr, Laura M. Judd, Summer J. Acker, Daniel L. Goldberg atmosphere, NO₂ has sharp concentration gradients with elevated levels that are both spatially and temporally proximate to its emission (Richmond-Bryant et al., 2018). From understanding the temporal and spatial patterns of tropospheric NO₂, we can better inform action to ameliorate the health burdens associated with NO₂.

The US EPA maintains a network of ambient air pollution monitors known as the Air Quality System (AQS) (https://www.epa.gov/aqs); these monitors measure hourly concentrations of criteria air pollutants including NO₂. AQS monitors measure surface-level concentrations with high fidelity that are important for regulatory purposes; however, they have known limitations. First, monitors are spatially constrained to a fixed point in space and thus they are unable to capture patterns in concentrations across large spatial areas (Cordioli et al., 2017). Additionally, a majority of AQS monitors are located in population dense areas in the East Coast and California. This spatial overrepresentation presents a challenge for characterizing NO₂ levels in regions with limited ground-level monitoring. Lastly, there is a known high bias in NO₂ observations that is attributable to the chemiluminescent monitors that are used throughout the AQS (Dickerson et al., 2019; Lamsal et al., 2008) in which monitors attribute concentrations of other reactive nitrogen species to NO₂. With these limitations in mind, previous analyses of monitoring and modeling have characterized NO₂ across different conditions. For example, previous work found seasonally consistent local minima in the midday and maxima in the morning and evening (Appel et al., 2017) that vertical column densities (VCDs) lag surface-level concentrations of NO₂ near road systems (Kimbrough et al., 2017).

Satellite remote sensing of NO₂ has become a widely adopted tool over the last few decades to provide spatially comprehensive observations that effectively fill monitoring network gaps. Remote sensing instruments such as the ozone monitoring instrument (OMI) and the TROPOspheric Monitoring Instrument (TROPOMI) observe atmospheric columns of trace gases including NO2 (Levelt et al., 2018; Veefkind et al., 2012). They measure reflected solar radiation in an NO₂ absorption wavelength region (405–465 nm) and use spectrometry algorithms to estimate NO₂ slant column densities. These slant columns are further converted to tropospheric vertical column densities through the application of an air mass factor (AMF) (Lorente et al., 2017a; Palmer et al., 2001), which require prior assumptions such as surface reflectivity, cloud height and coverage, and the vertical distribution of the retrieved trace gas. These remote sensing column observations are not equivalent to surface-level observations; however, they have been found to be positively correlated with monitor observations especially across longer timescales (Goldberg et al., 2021; Lamsal et al., 2014). Previous correlations were derived from early afternoon patterns—given the limited overpass times of these instruments—and thus the agreement between surface-level and remote sensing observations diurnally still remains poorly understood. Through the application of deterministic (e.g., Cooper et al., 2020) and statistical modeling (e.g., Larkin et al., 2023) surface-level NO₂ can be inferred from these remote sensing observations to enhance correlation; however, inclusion of diurnal patterns in these modeling approaches still needs to be tested.

There are distinct sampling strategy differences between remote sensing from low Earth orbiting (LEO) satellites versus Geostationary (GEO) orbiting satellites. LEO instruments only observe NO₂ once per day—for the case of OMI and TROPOMI this is in the early afternoon local time—and have globally complete coverage (Judd et al., 2018; Levelt et al., 2018; Veefkind et al., 2012). In contrast, GEO instruments such as those that are a part of the GEO-Ring for Air Quality: the Geostationary Environment Monitoring Spectrometer (GEMS), the NASA Tropospheric Emissions: Monitoring of POllution (TEMPO), and the European Space Agency Sentinel-4 mission are fixed in space relative to the Earth and are able to observe NO₂ with greater temporal detail (i.e., ~hourly, during daytime hours of approximately 8:00–17:00 LT) over a more limited spatial coverage (Yang et al., 2024a; Zoogman et al., 2017). As the GEMS satellite has been operational since February 2020, there have been a number of studies comparing GEMS column NO₂ to surface-level concentrations. One study found that across four regions in China (Li et al., 2023), GEMS column NO₂ had a correlation of 0.57 with surface-level NO₂ whereas analyses over Korea identified a stronger spatial correlation than temporal (Lee et al., 2024). Another study (Yang et al., 2024b) investigated the drivers of diurnal NO₂ in Beijing and Seoul and attributed increasing NO₂ throughout the day in the winter due to elevated daytime emissions and entrainment of O₃ and a minimum in the early afternoon driven by transport and chemical loss.

TEMPO began observing hourly NO_2 in North America in August 2023; it observes column NO_2 at unprecedented spatial and temporal resolution with relevance for uncovering diurnal and seasonal patterns in NO_2 (Zoogman et al., 2017) in the US. TEMPO tropospheric vertical column densities are calculated by applying an

NAWAZ ET AL. 2 of 22



AMF to the slant column densities. This AMF is derived using meteorological variables and trace gas vertical profiles from the GEOS Composition Forecasting (GEOS-CF) model (Keller et al., 2021) with a horizontal resolution of $0.25^{\circ} \times 0.25^{\circ}$, a geometry-dependent Lambertian equivalent reflectance (GLER) albedo, and cloud coverage information from the TEMPO CLDO4 product (González Abad et al., 2024b; Nowlan et al., 2025). Given the planned launches of other GEO instruments such as Sentinel-4 over Europe (Courrèges-Lacoste et al., 2017) and the NOAA GeoXO ACX instrument over the US (Lindsey et al., 2024), considering how GEO satellite remote sensing retrievals compare to surface-level monitoring is especially valuable for better understanding air quality.

In this study, we explore how temporally averaged estimates of NO_2 columns from TEMPO compare to surface-level observations from the US EPA AQS; this subject remains understudied given the novelty of TEMPO and geostationary measurements of this type. We leverage these TEMPO data, ground-level monitoring, and ERA5 meteorology reanalysis data (Hersbach et al., 2020), from August 2023 to August 2024 along with land use information. Specifically, we investigate how TEMPO NO_2 columns are correlated with surface-level monitor observations and consider how different characteristics—that is, diurnal patterns, seasonality, meteorology, and road proximity—affect these results. By considering these data, we identify the specific conditions under which TEMPO remote sensing is well and poorly aligned with surface monitoring. Lastly, we provide recommendations for modeling or estimating surface-level NO_2 with consequences for health analyses that are informed from the findings of our comparative analysis.

2. Methodology

In this study, we explore the relationship between long-term averaged hourly TEMPO tropospheric NO_2 columns and surface-level NO_2 concentrations from the EPA AQS for the August 2023 through August 2024 timeframe. We download hourly L2 TEMPO V03 overpasses across the US and spatially and temporally average them to capture hourly monthly averaged NO_2 at fine resolution $(0.01^\circ \times 0.01^\circ)$ across the continental US (CONUS). We additionally download hourly surface-level NO_2 from US EPA AQS monitors and average them to match the temporal resolution of the TEMPO observations. These data are compared directly for different times of the day, seasons, and based on their proximity to major roadways. Lastly, meteorological data are sourced from the ERA5 reanalysis product to explore how comparisons between column and surface-level NO_2 evolve across different meteorological conditions. The methods involved in these analyses are discussed in greater detail over the next sections.

2.1. US EPA AQS Surface-Level NO2

The US EPA AQS network contains monitors that measure ambient concentrations of the six criteria air pollutants including the focus of this study, NO_2 , at fixed locations near the surface. The temporal resolution and coverage of NO_2 observations vary across the network; however, in this study, we consider hourly concentrations of NO_2 . The US EPA validates and groups hourly concentrations of NO_2 from all AQS monitors as part of their pregenerated files (U.S. Environmental Protection Agency, 2025). We download these data for the time period of August 2023–August 2024 and use these for our analysis.

Ultimately, we consider 44,529 unique monthly average hourly NO₂ concentrations for 454 monitors across the US from the EPA AQS hourly data. We note that there are distinct classes of monitoring instruments in the AQS (i.e., chemiluminescent monitors and Cavity Attenuated Phase Shift or "CAPS" monitors); in our analysis, all of our results are calculated by combining observations from both types of monitors; however, we separately calculate statistics for the chemiluminescent and CAPS monitors as discussed in Section 3.1. When separating by monitor type, we find stronger correlation between ground-level observations and column NO₂ in the chemiluminescent monitors ($R^2 = 0.45$) than the CAPS instruments ($R^2 = 0.27$) despite comparable dynamic ranges of 40.7 and 40.6 ppb, respectively. This is surprising given that the chemiluminescent monitors have a known high bias from counting other reactive nitrogen species as NO₂ (Dickerson et al., 2019; Lamsal et al., 2008); however, we note that there are fewer CAPS monitors overall and that there are relatively more CAPS in the eastern US than chemiluminescent monitors and proportionally more near major roads (Figure S1 in Supporting Information S1) that could be responsible for this weaker correlation. Additionally, we compared nine collocated CAPS and chemiluminescent monitors and found generally strong correlation ranging from $R^2 = 0.91$ to 1.00, and no

NAWAZ ET AL. 3 of 22



systematic bias with slopes ranging from 0.82 to 1.00 and intercepts ranging from -1.00 to 0.71 ppb. These values indicate that the weaker correlation in CAPS is likely not attributable to the instrumentation specifically.

Monitors in the AQS can be sited in unique environments that are not necessarily representative of community surface-level NO_2 that should be considered when interpreting their results. A subset (15%) of these monitors are part of the "near-road monitoring network" (US EPA, 2020) and they are often located within 20 m of 6+ lane highways. Given that near-road monitors measure unique diurnal and seasonal patterns in NO_2 concentrations, we incorporate the EPA designation of "near-road" monitors in our analysis and then match TEMPO observations to these data. We note that there are regions that have been previously identified as over- and under-represented in this data set (Nawaz et al., 2025); specifically, monitors are predominantly located in the eastern US and California and in urban areas.

2.2. NASA TEMPO Column NO₂

The NASA Tropospheric Emissions Measuring of Pollution (TEMPO) instrument is a UV-visible spectrometer that observes atmospheric trace gases, including NO_2 , from space. It is positioned on a commercial satellite in a geostationary orbit that enables measurements over much of North America (68°W–13°W and 14°N–73°N) approximately once every hour. Depending on the viewing zenith angle, TEMPO has a spatial resolution that varies from around 8 km² over Mexico City to 21 km² over parts of Canada with a footprint of $\sim 2 \times 4.75$ km² at the center of the field of regard (Nowlan et al., 2025). The TEMPO observed spectra are fit to a modeled radiance through a least squares minimization to retrieve slant column densities (SCDs) of NO_2 . Columns are separated into stratospheric and tropospheric components as discussed in previous work (Geddes et al., 2018). These SCDs are then converted to tropospheric vertical column densities (VCDs) following previous methods derived for the ozone monitoring instrument (OMI) (G. González Abad et al., 2015). Hourly observations of NO_2 SCDs and VCDs are available during daylight hours at an unprecedented combined spatial resolution (i.e., $\sim 2 \times 4.75$ km²) and coverage (i.e., the CONUS) (Nowlan et al., 2025).

We download hourly TEMPO NO₂ SCDs and VCDs from the V03 algorithm during 2 August 2023–31 August 2024 (NASA/LARC/SD/ASDC, n.d.). These data are filtered to remove data affected by cloud coverage by only considering observations taken during an effective cloud fraction of less than 0.15 and the main data quality flags are equal to 0. After filtering, the data are regridded or "oversampled" to a 0.01° × 0.01° resolution to create "Level-3" data following previous work (Goldberg et al., 2021). The oversampling approach is also illustrated in a diagram in the supplement (Figure S2 in Supporting Information S1). Single pixel TEMPO NO₂ uncertainties have been estimated to be in the range of 15%–20% in polluted areas (Glissenaar et al., 2025). Oversampling the NO₂ observations, as we do in this work, sacrifices information on the daily variability of NO₂ to reduce uncertainty and generate longer-timescale estimates at finer spatial resolution. However, in this analysis, we preserve the hourly variation while losing the day-to-day variance to generate monthly average hourly TEMPO data. We conduct our analysis for monthly and annually averaged TEMPO data, as opposed to daily data, because of the stronger epidemiological link between longer-term NO₂ exposure and chronic health conditions, such as asthma (GBD 2021 Risk Factor Collaborators, 2024) and to reduce variability. Throughout this study, our TEMPO results are presented for the VCDs, as opposed to the SCDs, unless otherwise specified and when discussing VCDs, we are specifically referring to the tropospheric VCDs—not the total columns.

2.3. ERA5 Meteorological Reanalysis Data

The European Centre for Medium-Range Weather Forecasts (ECMWF) maintains the ERA5 reanalysis data set that assimilates atmospheric observations using a 4D-Var assimilation approach to provide hourly estimates of different atmospheric characteristics (Hersbach et al., 2020). These meteorological data are presented for 137 vertical levels interpolated to key specific heights at a $0.25^{\circ} \times 0.25^{\circ}$ horizontal spatial resolution; temporally, these data are generated in near-real time at an hourly resolution. They are aggregated to different temporal averages including a monthly average by hour of the day that is comparable to the monthly averaged hourly NO₂ columns and concentrations that we calculate for TEMPO and AQS observations.

Given its relatively short atmospheric lifetime, surface, and column NO_2 are especially dependent on near-surface meteorological characteristics such as the boundary layer height (BLH) and advection; we incorporate ERA5 data to consider how NO_2 —and correlations between the surface and column—vary across different meteorological conditions. We begin by downloading the monthly average by hour of day data for BLH and 10-m wind speeds

NAWAZ ET AL. 4 of 22



from August 2023-August 2024, inclusive. We align our TEMPO data with the ERA5 meteorological data by location, hour-of-the-day, and month of the year; however, given that we are conducting our analysis at the monthly timescale, we do not capture daily variability. Thus, our meteorological analyses are more representative of longer-term seasonal changes as opposed to distinct responses to short-term events. For each observation, we identify the month and hour in GMT and the ERA5 grid cell in which the monitor is located to match the meteorological characteristics to specific NO₂ observations. In doing so, we correspond the monthly average hourly BLH and wind speeds to the associated NO₂ observation.

2.4. Urban Boundary and Road-Proximity Land-Use Data

In our analysis, we leverage land-use data to identify monitor location characteristics that could influence NO_2 levels and comparisons between surface and column NO_2 . To characterize urban areas, we use urban boundary information from the 2023 Global Human Settlement Grid (GHS-SMOD) for approximately 11,000 cities globally ("European Commission," 2025). The GHS-SMOD product identifies urban centers by considering contiguous grid cells with high population density that have greater than 50,000 inhabitants; it leverages remote sensing data to characterize these urban centers at fine resolution (i.e., $1 \times 1 \text{ km}^2$) that is aligned with our TEMPO data. We calculate urban city centers for our meteorology analysis (refer to Section 2.3) by applying the built-in centroid function from the GeoPandas python package (GeoPandas Development Team, 2025) to the GHS-SMOD shapefile for individual urban boundaries. Additionally, monitors were classified by their proximity to roadways using distance buffers applied to the combined state-level Census Bureau 2021 Tiger/Line Primary and Secondary Roads shapefiles for the entire CONUS. We created four distance buffers: less than 50 m, 50–300 m, 300 m to 1 mile, and greater than 1 mile. Monitor locations were then spatially merged with these buffers to assign each monitor to the appropriate distance category. We note that this road proximity classification is distinct from the US EPA classification and is only considered in Section 3.2.

2.5. Comparative Analysis

After downloading the AOS and TEMPO data—and processing them independently as discussed above—we perform our comparative analysis. First, we identify each monitor through its distinct AQS ID by combining the state code, county code, and instrument ID to avoid combining observations from multiple instruments located at the same latitude and longitude. Occasionally, multiple observations were taken at a single site for the same hour and date; in these cases, we calculate the mean 1-hr average value. In order for it to be appropriate to average these collocated monitors, their observations should be highly correlated. To explore this, we calculated correlation between the hourly observations at the nine locations with multiple monitors (Figure S3 in Supporting Information S1) and found that across all sites, observations were well correlated (ranging from $R^2 = 0.91$ to $R^2 = 1.00$). We identify the day, month, and year an observation was taken based on the GMT date and average across all the days for each unique month and year pair to calculate monthly averaged hourly surface-level concentrations; observations from monitors that had 15 or fewer observations for a given month-hour pair were removed. Additionally, we remove monthly average observations for which TEMPO data are unavailable. After processing the hourly TEMPO data to the monthly averaged hourly timeframe and the variable spatial resolution to the fixed $0.01^{\circ} \times 0.01^{\circ}$ grid, these TEMPO column NO₂ observations are matched to the surfacelevel AQS NO₂ observations. First, TEMPO and AQS NO₂ are grouped for each combination of month and hour —in GMT. After temporally matching these two data sets, for each monitor, we identify the $0.01^{\circ} \times 0.01^{\circ}$ TEMPO grid cell in which the monitor is located. We use the corresponding TEMPO data from that grid cell to identify the column NO₂ for the specific month, hour, and monitor location for comparative purposes. In doing so, we match monthly averaged TEMPO column NO2 and AQS surface-level NO2 for the same approximate temporal and spatial point and conduct our comparative analysis.

Oversampling NO_2 observations, as we do in this work, sacrifices information on the daily variability of NO_2 to improve precision and generate longer-timescale estimates at finer spatial resolution. However, in this analysis, we preserve the hourly variation while losing the day-to-day variance to generate monthly average hourly TEMPO data. We explore the relationship between AQS surface-level and TEMPO column NO_2 through a series of sub-setting, aggregating, and processing steps. For all the results presented in this study, we identify the hour of the day using LT not GMT. Seasonally, we perform calculations for the Winter (December, January, and February), Spring (March, April, and May), Summer (June, July, and August), and Fall (September, October, and November).

NAWAZ ET AL. 5 of 22

We aggregate the data to compare AQS surface NO_2 to TEMPO column NO_2 for different averaging periods. The baseline level of aggregation is the monthly average hourly NO_2 (MAH) in which we calculate a monthly average NO_2 value for each hour of the day for every month between August 2023 and August 2024, inclusive. We also average across all months to calculate annual average hourly NO_2 (AAH), average across all hours to calculate the monthly daytime average (MDA), and average across all months and hours to calculate annual daytime average NO_2 (ADA). Lastly, we calculate monthly average hourly NO_2 in which we average across all monitors in the US (MAH US) removing spatial variability in our comparisons. These aggregations are calculated as follows:

$$z_{h,I}^{\text{AAH}} = \frac{\sum_{m} z_{m,h,I}^{\text{MAH}}}{N_{h,I}} \tag{1}$$

$$z_{m,I}^{\text{MDA}} = \frac{\sum_{h} z_{m,h,I}^{\text{MAH}}}{N_{mI}} \tag{2}$$

$$z_I^{\text{ADA}} = \frac{\sum_{m,h} z_{m,h,I}^{\text{MAH}}}{N_I} \tag{3}$$

$$z_{h,m}^{\text{MAH US}} = \frac{\sum_{I} z_{m,h,I}^{\text{MAH}}}{N_{m,h}} \tag{4}$$

Where $z_{m,h,I}^{\text{MAH}}$ refers to the monthly average hourly NO₂ at a monitor (I) and for an hour (h) and month (m) and N refers to the number of observations considering specific conditions (e.g., $N_{h,I}$ is the number of observations for a single monitor and hour).

For several steps in our analysis, we apply a standardization to ensure that TEMPO and AQS data are normalized in a manner that is independent of their units. To calculate these standardized NO_2 values, we first scale the TEMPO data by a factor of 10^{15} , as tropospheric column NO_2 typically fall within this order of magnitude. Then, for both the AQS and TEMPO data, we calculate the mean and standard deviation, and for all data, we subtract off the mean and divide by the standard deviation. In our analysis, we characterize the slope and correlation between surface-level and column NO_2 by calculating a least-squares linear regression. We use this standardized NO_2 to identify correlations between TEMPO and AQS across different meteorological conditions; however, dynamic ranges of all monthly averaged data are calculated for the unstandardized levels as follows:

Dynamic Range =
$$max(z) - min(z)$$
 (5)

Where z refers to the NO_2 levels—that is, TEMPO columns or AQS concentrations—for which we are calculating the dynamic range. A small dynamic range will often be linked with poor correlation; for these smaller ranges, TEMPO pixel and AQS instrument uncertainty have a greater influence on our comparative analysis that leads to degraded correlation. Therefore, this calculation is helpful in correlation comparisons to ensure conclusions drawn are only for locations and times that measure considerably above the observational uncertainty—that is, an upper bound of around 1×10^{15} molecules cm⁻² for TEMPO (Nowlan et al., 2025).

When considering how meteorology and road proximity influence the relationship between NO_2 and surface to column correlation, we bin the NO_2 data. To do so, we group NO_2 concentrations based on the specific parameter (e.g., BLH) into different bins based on the parameter values. For the BLH and wind data, we determined the data binning into equal-frequency deciles based on the following criteria: we selected the largest number of bins for which the correlation did not vary substantially between adjacent bins. For more than 10 bins there began to be large shifts in correlation between adjacent bins for these two meteorological conditions; however, a fewer number of bins would lose some degree of detail in the distribution. For the road proximity analysis, the data were already categorized into road distance groups, and so, we chose these for the binning. After binning the data, we generate box-whisker plots that present the mean and the inner quartiles of data with whiskers extending to the ends of the distribution ignoring data points identified as outliers (i.e., values that are further than 1.5 IQR of Q3 and Q1).

NAWAZ ET AL. 6 of 22

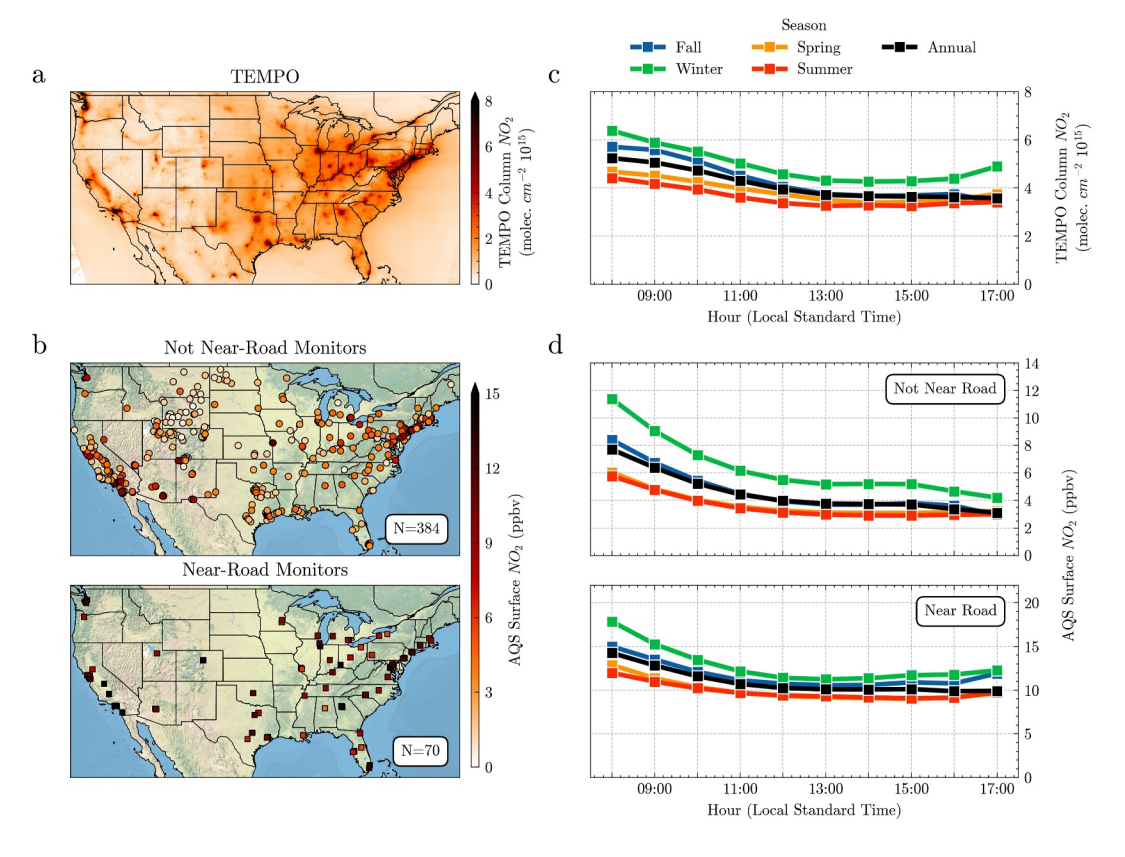


Figure 1. (a) Distribution of annual-average equivalent (August 2023–August 2024) daytime TEMPO Column NO_2 across the CONUS. (b) EPA AQS monitor NO_2 annual average concentrations for not near road (top) and near road (bottom) monitors. Monitors are distinguished by marker shape as being "near road" or "not near road" based on the EPA near road classification with squares and circles, respectively. (c) Diurnal profiles of annual averaged TEMPO column NO_2 for data coincident with AQS monitors annually and for specific seasons averaged across all monitors. (d) AQS surface-level NO_2 for not near road monitors (top) and near road monitors (bottom).

3. Results

3.1. Spatial, Diurnal, and Seasonal Correlations Between TEMPO and Surface-Level NO2

Column measurements from TEMPO reveal daytime NO₂ at an unprecedented combined spatial coverage and temporal resolution across the CONUS. TEMPO annual average equivalent columns from August 2023 to August 2024 characterize NO₂ levels both in areas with extensive AQS coverage and in gaps in the monitoring network (Figure 1a). Monitors from the AQS are predominantly located in the northeastern US and California (Figure 1b). Additionally, 49% and 27% of these monitors were located within cities and outside of cities but within 50 km, respectively, of one of the 189 unique US urban areas identified using GHS-SMOD urban boundaries ("European Commission," 2025). TEMPO observations reveal NO₂ hotspots in areas that lack sufficient AQS surface-level monitors: for example, the Permian Basin in western Texas and the city of Omaha, Nebraska.

Column measurements from TEMPO not only provide enhanced spatial detail of NO_2 levels in the CONUS but also enable the exploration of diurnal patterns in NO_2 columns (Figure 1c). TEMPO columns—spatially and monthly averaged—decrease from 5.2×10^{15} molecules cm⁻² at 8:00 to stabilize at 3.6×10^{15} molecules cm⁻² between 15:00 and 17:00 LT ultimately decreasing by 31%. This morning to afternoon decrease is sharper in the Fall (37%) and Winter (29%) than the Summer (24%) and Spring (24%). Diurnal patterns in AQS surface-level NO_2 (Figure 1d) deviate from TEMPO: overall for the same hours, AQS concentrations decrease by 49% at the annual scale and by 53%, 50%, 42%, and 42% for the Fall, Winter, Summer, and Spring, respectively. Additionally, from 8:00 to 9:00 LT, AQS surface-level NO_2 decreases both at near road sites (-10.0%) and not near road sites (-17.3%); however, the decrease in TEMPO column NO_2 is more gradual between these 2 hours at -3.4%, which could potentially be driven by BLH dynamics. We anticipated this difference between the temporal

NAWAZ ET AL. 7 of 22



patterns in the column and surface NO₂ as they respond differently to changing BLH dynamics; previous work (Yang et al., 2024b) has noted that diurnal patterns in surface-level NO₂ are generally more responsive to variability in mixing depths than column NO₂.

This deviation in behavior may be attributable to BLH dynamics: as the BLH increases in the morning, surface level air is vertically mixed to higher altitudes and thus column NO₂ does not reflect changes in surface level concentrations. Although we restrict the AQS data to those aligned with TEMPO overpasses here, full diurnal profiles for all hours of the day are included in the supplement (Figure S4 in Supporting Information S1).

Toward the end of daylight hours (i.e., 17:00), surface-level NO_2 concentrations at near road sites demonstrate divergent behavior compared to not near road sites. Specifically, AQS surface-level NO_2 are relatively stable at near road sites and increase slightly by 0.4%; in contrast, they decrease by 7.9% at not near road sites. We note, however, that there is a greater representation of observations at 17:00 from the spring and summertime when NO_2 levels are lower. Thus, potential diurnal increases in NO_2 driven by increased traffic-related NO_x emissions and a decreased BLH is counteracted by a larger fraction of the 17:00 NO_2 coming from the spring and summer (Figures S5 and S6 in Supporting Information S1). To explore this, we additionally calculate the average NO_2 levels for all 24-hr of AQS data and do not filter by those that are coincident with TEMPO (Figure S4 in Supporting Information S1). In doing so, we see sharp increases in ground-level NO_2 between 16:00 and 17:00 annually and weaker increases in the spring and summer. To further unpack the influence of traffic patterns on NO_2 , it would be beneficial to explore weekday and weekend differences as we have done previously (Nawaz et al., 2024) in Houston; however, given that we exclusively focus on monthly average NO_2 in this analysis, as discussed in the methods, this is beyond the scope of this current work.

TEMPO and AQS monitors observe NO₂ from distinct perspectives that have implications for diurnal and spatial patterns that vary across different cities (Figure 2). We explore how spatial and diurnal patterns differ between TEMPO column NO₂ and AQS surface-level NO₂ within five of the largest metropolitan areas in the US—New York, Washington, Chicago, Houston, and Los Angeles. In the morning (i.e., from 8:00 and 12:00 LT), AQS surface-level NO₂ decreases sharply for each of the five cities: by 34.9% (New York), 44.6% (Washington), 35.8% (Chicago), 45.9% (Houston), and 36.0% (Los Angeles). In contrast, for this same period, TEMPO column NO₂ decreases more gradually for the five cities: by 6.0% (New York), 31.0% (Washington), 6.5% (Chicago), 20.1% (Houston), and 27.4% (Los Angeles). Thus, there is a clear decrease in AQS surface-level NO₂ in the morning for these five cities that is likely induced by increasing BLH. This increasing BLH allows NO₂ to more easily mix vertically with no associated change in the column amount by this cause alone. This is not universally true; for cities such as Los Angeles, diurnal patterns in column NO₂ match surface-level patterns relatively well. However, caution should be taken in applying TEMPO to infer diurnal patterns at the surface without considering the meteorological conditions (e.g., BLH and advection)—and the relationship of these with proximities to the urban sources that affect column and surface-level NO₂ differently.

In these five cities, diurnal patterns in TEMPO column and AQS surface-level NO $_2$ have the most similar patterns in the late morning and early afternoon (i.e., between 11:00 and 15:00 LT). Toward the end of the day (i.e., between 15:00 and 17:00 LT), however, TEMPO and AQS observe city-specific changes in NO $_2$ levels. Specifically, in this late afternoon period, AQS surface-level NO $_2$ changes by -3.7% (New York), +4.4% (Washington), +2.2% (Chicago), -9.5% (Houston), and -19.0% (Los Angeles). In contrast, for this same time period, TEMPO diurnal patterns vary by -22.9% (New York), -4.5% (Washington), -4.9% (Chicago), +13.7% (Houston), and +6.2% (Los Angeles). These divergent patterns in NO $_2$ levels toward the end of the day suggest that TEMPO tropospheric vertical columns are unable to consistently capture surface-level shifts in NO $_2$ levels in the late afternoon for specific cities; however, we note that these differences could partially be exacerbated from our inclusion of near road monitoring data in this analysis. For a similar set of cities, a prior study (Penn & Holloway, 2020) found generally consistent behavior in that surface-level NO $_2$ decreased more sharply from the morning to the afternoon (between 1.5 and 3 times higher in the morning) than remote sensing (1.2–1.8).

We explore the relationship between TEMPO column and AQS surface-level NO_2 concentrations further by standardizing the two data sets and calculating a least-squares linear regression to derive the coefficient of determination (R^2) and slopes between the two (for details refer to Section 2.5). We note that since surface-level and column NO_2 are two distinct methods of observation—that is, tropospheric column NO_2 represents the integrated amount of NO_2 from the surface to the tropopause whereas the surface NO_2 measures the local concentration near ground-level—there is an upper limit to how well correlated they can be. This standardization is

NAWAZ ET AL. 8 of 22

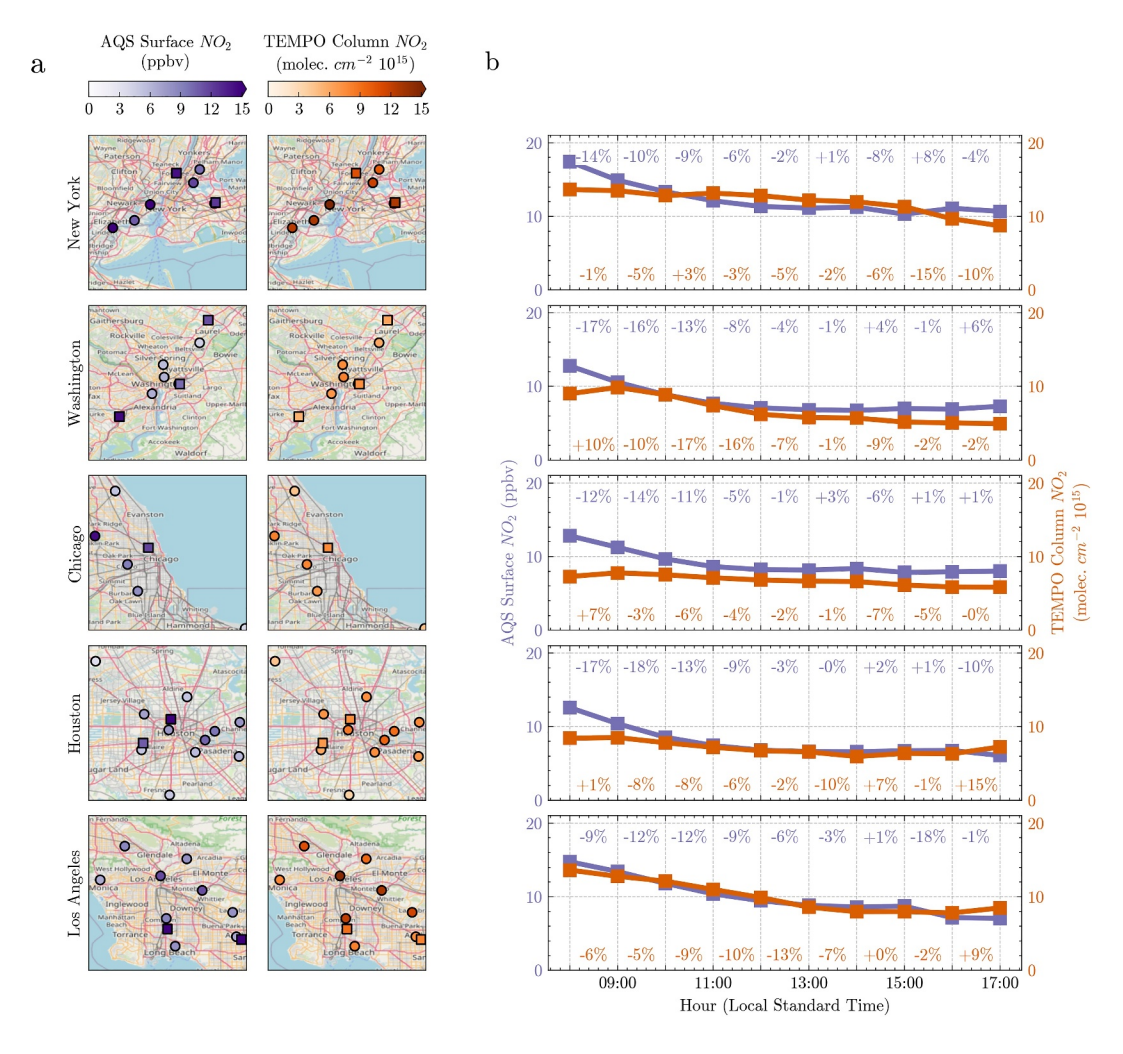


Figure 2. (a) Annual-average equivalent (August 2023–August 2024) daytime EPA AQS surface-level concentrations (left) and TEMPO Column NO₂ (right) across five major metropolitan areas—New York, Washington, Chicago, Houston, and Los Angeles. Monitors are distinguished by marker shape as being "near road" or "not near road" based on the EPA near road classification as squares and circles, respectively. (b) Diurnal profile of annual average TEMPO column NO₂ (orange) and AQS surface-level NO₂ (purple) in the same five cities across all monitor locations for each city included in (a) with the hourly percent changes in AQS (purple) and TEMPO (orange) included for each city.

done both overall and for specific times of the day, seasons, and near road classifications (Figure 3). Across all monthly averaged hourly (MAH) NO₂ data, TEMPO columns are moderately correlated ($R^2 = 0.42$) with AQS surface-level concentrations. Column and surface-level MAH NO₂ are better correlated in the morning ($R^2 = 0.45$) and correlations degrade through the early ($R^2 = 0.37$) and late ($R^2 = 0.28$) afternoon as the BLH increases and vertical mixing is enhanced. This is driven in part by smaller dynamic ranges in the TEMPO data in the early afternoon (27.2 × 10¹⁵ molecules cm⁻²) and late afternoon (27.3) compared to the morning (40.7). In contrast, AQS monitors have ranges that are stable varying from 38.4 ppb in the morning to 39.2 in the late afternoon. The agreement between TEMPO and AQS also varies by season. TEMPO column and AQS surface-level MAH NO₂ are better correlated in the Fall ($R^2 = 0.46$) and Winter ($R^2 = 0.41$) than the Spring ($R^2 = 0.37$) and Summer ($R^2 = 0.38$) but notably, TEMPO data have a greater range in the Fall (34.4 × 10¹⁵ molecules cm⁻²) and Winter (40.7) than the Spring (25.5) and Summer (31.2). Here, we present results that include observations from both chemiluminescent and CAPS instruments; however, we note that agreement deviates for these two types of monitors (Figures S7 and S8 in Supporting Information S1). Specifically, TEMPO is better correlated with chemiluminescent observations ($R^2 = 0.45$) than CAPS ($R^2 = 0.27$); however, there are more monitors of the prior type ($R^2 = 0.36$) than the latter ($R^2 = 0.45$) than CAPS ($R^2 = 0.27$); however, there are more monitors of the prior type ($R^2 = 0.36$) than the latter ($R^2 = 0.45$) than CAPS ($R^2 = 0.27$); however, there are more monitors of the

NAWAZ ET AL. 9 of 22

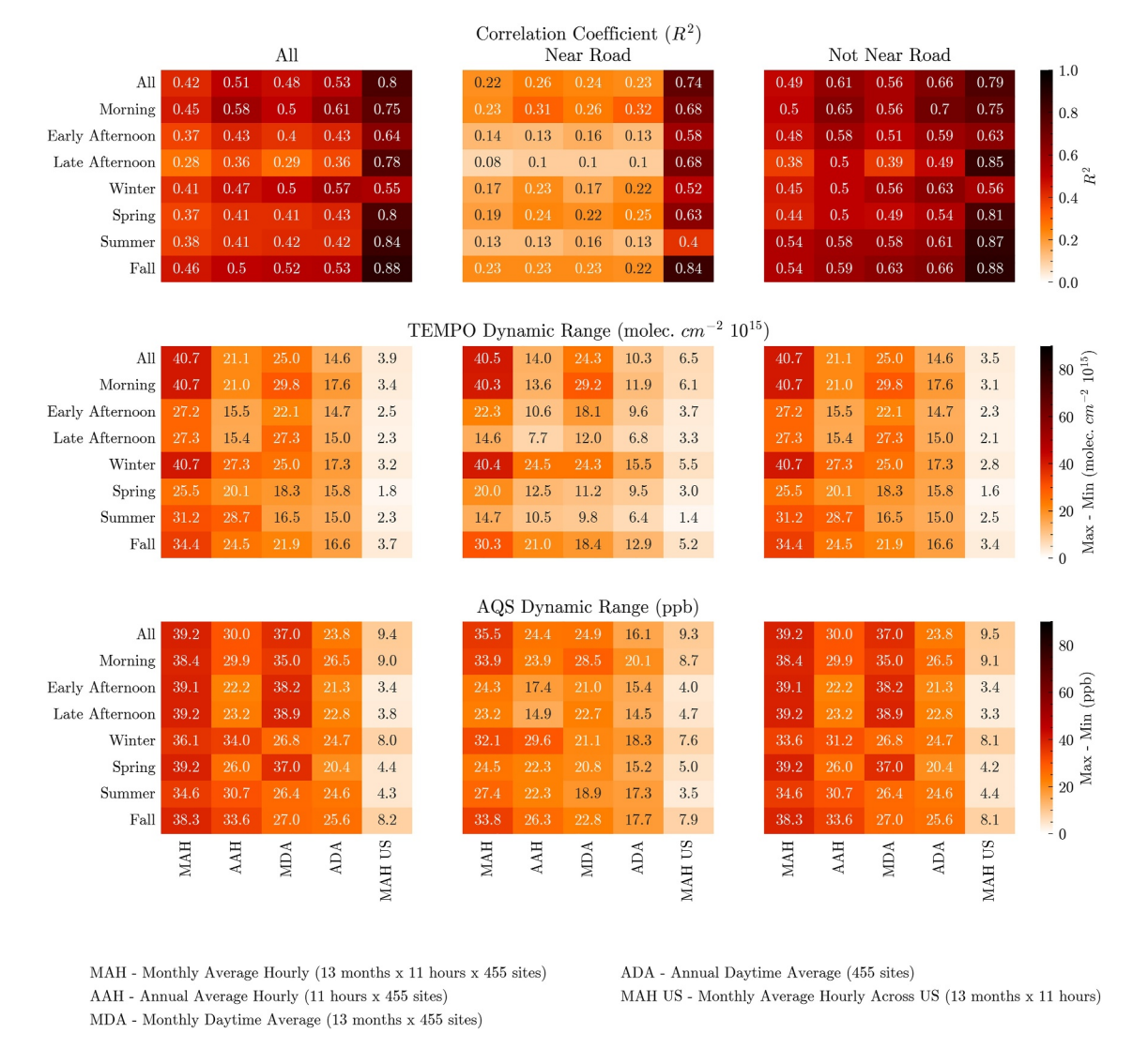


Figure 3. (top) Correlation coefficients across different diurnal and seasonal subgroups (rows) and for different averaging groups (columns). Correlations are calculated separately for all monitors (top left), near road monitors (top middle), and monitors not near road (top right) based on the EPA classification. (middle) The dynamic range of TEMPO and (bottom) AQS. Here, morning refers to 8:00–11:00 LT, early afternoon refers to 12:00–14:00 LT, and late afternoon refers to 15:00–17:00 LT.

Correlations between surface-level and column NO_2 vary dependent on the degrees of averaging applied to the concentrations. When monthly variability is removed in the calculation of the annual average hourly NO_2 (AAH), correlation between TEMPO and AQS NO_2 improves ($R^2 = 0.51$) compared to the MAH ($R^2 = 0.42$) and also the monthly daytime average (MDA) ($R^2 = 0.48$) in which hourly variation is removed despite having a lower dynamic range (21.1×10^{15} molecules cm⁻²) than the MAH (40.7) and MDA (25.0) for TEMPO. This suggests that averaging over seasonal variation enhances correlation between column and surface-level NO_2 more than averaging over diurnal variation, which is consistent with expectations as column and surface NO_2 exhibit distinct diurnal patterns. When both monthly and seasonal variation are removed in the annual daytime average (ADA), correlation again improves further ($R^2 = 0.53$). Lastly, we consider the implications of removing spatial variation by averaging across all monitors in the US to quantify monthly average hourly NO_2 across the US (MAH US). When spatial variability is removed and only seasonal and diurnal variation are considered, TEMPO and AQS NO_2 are well correlated ($R^2 = 0.80$).

The prior paragraphs focused on correlations across all monitors; however, we find divergent patterns in correlation when distinguishing the monitors that are near major roads from those that are not. At not near road monitors, TEMPO column and AQS surface-level MAH NO_2 are better correlated ($R^2 = 0.49$) than those that are

NAWAZ ET AL. 10 of 22



near road ($R^2 = 0.22$) despite comparable dynamic ranges in the prior (40.7×10^{15} molecules cm⁻²) and the latter (40.5) for TEMPO. This suggests that TEMPO columns likely are more reliable at representing surface-level NO₂ concentrations at locations that are not directly adjacent to major roads and their associated sharp gradients in NO₂ levels. Although near road and not near road monitors exhibit similar patterns in TEMPO and AQS correlation at different times of day and across different seasons, there are some notable exceptions. Correlations drop more dramatically throughout the course of the day at near road monitors from the morning ($R^2 = 0.23$) to the early afternoon ($R^2 = 0.14$) and bottoming out in the late afternoon ($R^2 = 0.08$). In contrast, at the not near road monitors, correlations are stable in the morning $(R^2 = 0.5)$ and early afternoon $(R^2 = 0.48)$ before worsening in the late afternoon ($R^2 = 0.38$). Considering seasonality, near road monitors have the strongest correlations in the Fall $(R^2 = 0.23)$ and Spring $(R^2 = 0.19)$ in contrast to the not near road monitors for which correlations are strongest in the Fall ($R^2 = 0.54$) and Summer ($R^2 = 0.54$). Applying different averaging to the NO₂ columns and concentrations also affects correlation at near road and not near road monitors distinctly. Most notably, when averaging out seasonal and diurnal variation in the ADA, correlation between surface and column NO2 is much stronger at the not near road monitors ($R^2 = 0.66$) than the near road monitors ($R^2 = 0.23$). This is anticipated as the not near road monitors represent less variable NO₂ levels that are more aligned with the diffuse gridded TEMPO data than the near road monitors.

As a sensitivity analysis, we calculate the correlations between TEMPO column and AQS surface-level NO₂ at a 1-hr positive and negative lag (Figures S9 and S10 in Supporting Information S1) to compare to previous work (Harkey & Holloway, 2024) that found that VCDs lag surface-level concentrations by around 1 hr in the morning. When a 1-hr negative lag is applied to the TEMPO column NO₂ (e.g., TEMPO observations at 9:00 LT are assigned to 8:00 LT), correlations between column and surface-level NO₂ overall are similar and slightly increase in the morning while worsening in the afternoon. This is consistent with prior work (Harkey & Holloway, 2024) that found that morning VCDs lag surface concentrations by 1 hr on average. When a 1-hr positive lag is applied to TEMPO, column to surface-level correlations are notably worse throughout. Additionally, we characterize correlations separately for those within urban boundaries and not within urban boundaries (Figure S11 in Supporting Information S1) and note that near-road correlations are especially degraded for monitors located within urban boundaries.

Patterns in the correlation between TEMPO column and AQS surface-level NO2 are further examined by comparing them across individual hours, months, and monitors (Figure 4). Considering correlation at individual monitors, values varied from $R^2 = 0.00$ (30-083-0002; Andes, MT) to $R^2 = 0.91$ (49-013-7011; Uinta Basin, UT) (Figure 4a); however, we note that poor correlation at the Andes, MT site is likely driven by its small dynamic range (4.4 ppb and 2.2×10^{15} molecules cm⁻² for AQS and TEMPO, respectively). Restricting monitors to those with high dynamic ranges (classified as >20 ppb AQS NO₂), the poorest correlation of $R^2 = 0.00$ is found near Durango, CO (08-067-7003), which could implicate error associated with surface pressure, mountain breeze, or transient wildfire plumes. All but one of the eight states with the highest median correlations were located on the US East Coast ranging from $R^2 = 0.46$ in North Carolina to $R^2 = 0.55$ in Virginia (Table S1 in Supporting Information S1). In contrast, the worst performing states were mostly upper latitude states in the Pacific Northwest, Mountain West, and Midwest ranging from $R^2 = 0.01$ in Montana, North Dakota, and Colorado to $R^2 = 0.13$ in Idaho; however, these poor correlations are driven in part by low dynamic ranges for monitors in these states. Considering the least-squares regression slope values for TEMPO and AQS (Figure 4b), there are higher values in the East Coast US and California. We note that, given the difference in units and measurements between TEMPO column and AQS surface-level NO2, a slope of one does not necessarily represent the best agreement; instead, the slopes reflect how TEMPO data change with respect to changes in AQS data. For example, a higher slope indicates that TEMPO changes more dramatically per change in AQS.

Correlations and slopes between TEMPO column and AQS surface-level NO_2 are diurnally dependent (Figure 4d). In the early morning hours of 6:00 and 7:00 LT, correlations between TEMPO and AQS are weakest at $R^2 = 0.23$ and $R^2 = 0.35$, respectively. This could be due to fewer coincidences during these hours than others—there are 64% (06:00 LT) and 32% (07:00) fewer TEMPO observations than the average between 8:00 and 16:00 (Figure S6 in Supporting Information S1). Given that there are fewer observations taken during the early morning and evening, we note that the correlations at these times are likely less representative than during the rest of the day in which there are more observations. There are also geophysical reasons why uncertainty in the TEMPO retrievals may be higher during this time of day (González Abad et al., 2024a; Nowlan et al., 2025). Specifically, there is less sensitivity of the TEMPO instrument to near-surface pollution due to a longer sunlight path through

NAWAZ ET AL. 11 of 22

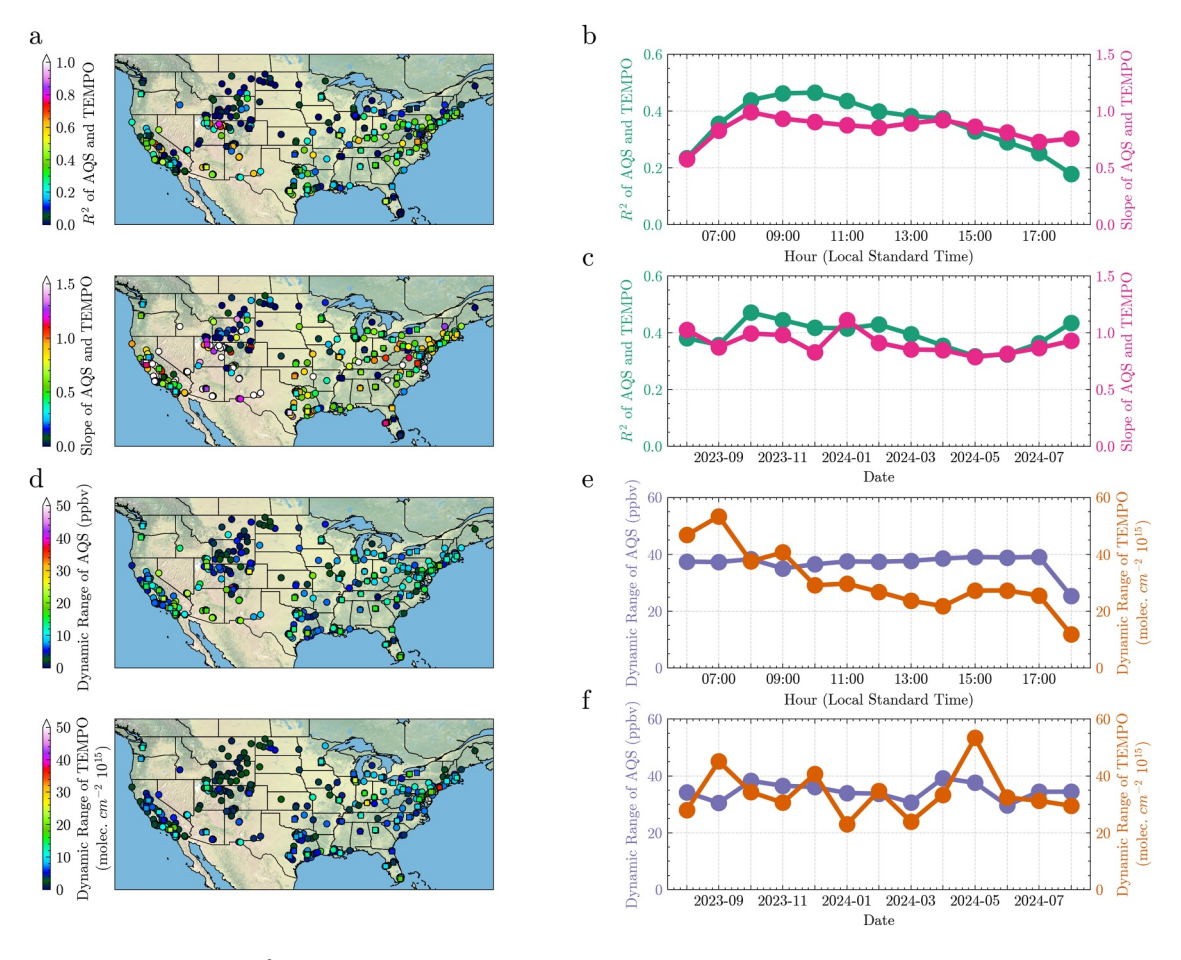


Figure 4. (a) Coefficient of Determination (R^2) (top) and slope (bottom) between the monthly average hourly TEMPO and AQS data for all individual monitors in the continental US. Coefficient of Determination (R^2) (green) and slope (pink) grouped by hour of day (b) and month (c). (d) Dynamic range in AQS and TEMPO for the AQS monitors. Dynamic range for AQS (purple) and TEMPO (orange) grouped by hour (e) and month (f).

the atmosphere and the subsequent increased sensitivity to retrieval assumptions. Additionally, observations at 6:00 LT are almost exclusively from the summer and spring months during which NO_2 levels are lower and correlations are weaker. Observations at 7:00 LT almost entirely exclude the wintertime and its associated elevated NO_2 levels (Figure S6 in Supporting Information S1). By 8:00 LT, and throughout the rest of the morning, correlations range from 0.40 to 0.46.

Correlations peak at around 10:00 LT and continue to decline throughout the afternoon until bottoming out at $R^2 = 0.17$ at 18:00 LT when the dynamic range of both TEMPO and AQS is minimized. When we decompose this analysis by season, we find that similar diurnal patterns occur in the Fall, Summer, and Spring; however, the wintertime exhibits a distinct diurnal profile in which correlations continue to increase throughout the morning and early afternoon until peaking at around 14:00 LT and subsequently dropping sharply (Figure S12 in Supporting Information S1). The diurnal profile of slopes between TEMPO and AQS follow the profile of correlations in the morning; however, slopes do not decrease as severely in the late afternoon hours. Ultimately, TEMPO NO_2 appears to be poorly correlated with surface-level NO_2 in the early morning and late afternoon and during these periods, we urge greater caution when attempting to derive information on surface-level patterns from these column observations. The seasonal dependence of the TEMPO and AQS NO_2 comparison is generally weaker (Figures 4e and 4f).

Throughout this study, when comparing TEMPO column to AQS surface-level NO_2 , we have exclusively considered the TEMPO tropospheric vertical column densities (VCDs); however, previous work has found that the application of AMFs to slant column densities (SCDs) to derive VCDs is the largest source of uncertainty in the algorithm (Lorente et al., 2017a) and little work has been done to characterize this uncertainty for

NAWAZ ET AL. 12 of 22

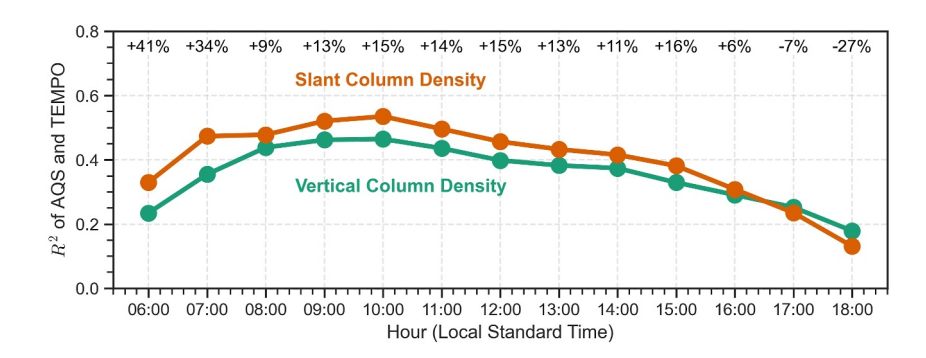


Figure 5. (a) Least-squares linear regression R^2 correlation between AQS observations and TEMPO slant column densities (orange) and vertical column densities (green) for each daytime hour. The percent to which slant column densities are higher or lower than vertical column densities is included at the top of the figure above each pair of points.

geostationary observations. To investigate how the AMF application could affect column to surface agreement, we characterize the correlations between TEMPO NO_2 VCDs and SCDs, compared to AQS surface-level NO_2 , as a function of hour of the day (Figure 5). Throughout most of the day, SCDs are better correlated with surface-level NO_2 . Starting in the early morning, SCDs have +41% and +34% higher R^2 at 6:00 and 7:00 LT than VCDs. For much of the rest of the day, SCDs have between +9% and +16% higher correlations (8:00 and 15:00 LT). After 16:00 LT, the correlations of SCDs and VCDs converge to similar values in which the SCDs are actually more poorly correlated (-7% and -27% at 17:00 and 18:00 LT) with AQS observations than the VCDs. Ultimately, throughout much of the day, SCDs are better correlated with surface-level NO_2 than VCDs; however, in the late afternoon and early evening, VCDs begin to have comparable, and even slightly stronger, correlation with surface-level NO_2 . As discussed in the previous paragraph, these diurnal patterns in correlation exhibit seasonal variability.

We note that SCDs are sensitive to the solar zenith angle and viewing zenith angle; to understand how these affect the correlation of SCDs with ground-level NO₂, we performed an additional analysis for a single month in which we apply a geometric AMF to the SCDs (Figure S13 in Supporting Information S1). The application of the geometric AMF slightly degraded correlation for this month, but this was a relatively minor impact and the SCDs with the geometric AMF applied still substantially outperformed the VCDs.

We further characterize the agreement of the SCDs with AQS observations by comparing TEMPO SCDs, TEMPO VCDs, and TROPOMI VCDs at the approximate time of TROPOMI overpass (\sim 13:00 LT) (Figure 6) for monthly and annually averaged data across the four distinct seasons. Generally, all three instruments perform comparably; however, the TEMPO SCDs are slightly better correlated ($R^2 = 0.55$) with surface-level NO₂ than the TROPOMI ($R^2 = 0.50$) and TEMPO ($R^2 = 0.48$) VCDs. At the annual timescale, TEMPO VCDs ($R^2 = 0.53$) slightly outperform TROPOMI VCDs ($R^2 = 0.51$) while still underperforming TEMPO SCDs ($R^2 = 0.57$). The performance of the TEMPO VCDs is especially poor at the near road monitors ($R^2 = 0.24$) compared to TROPOMI VCDs ($R^2 = 0.36$) and TEMPO SCDs ($R^2 = 0.44$), indicating that the application of the AMF for TEMPO especially degrades correlation at these sites. Future evaluations of new retrieval versions from TEMPO could consider comparing results of SCDs versus VCDs relative to reference measurements as a metric for how much uncertainty in the products can be attributed to the AMF.

3.2. Meteorological and Road Proximity Effects on Correlation Between TEMPO Column NO_2 and AQS Surface-Level NO_2

Meteorological conditions affect column and surface NO_2 differently with implications for correlation between TEMPO and AQS observations. We explore the influence of meteorology on NO_2 by characterizing how TEMPO column and AQS surface-level NO_2 vary across different BLHs (Hersbach et al., 2020) and quantify how this variation impacts correlation (Figure 7). Previous work (Choi et al., 2020; Flynn et al., 2014) characterized the diurnal variation in the vertical distribution of NO_2 in the boundary layer; they found that NO_2 levels generally decrease with increasing altitude. They find that NO_2 can accumulate at around approximately a third of the boundary layer height depending on the season and location. We consider the influence of meteorology distinctly for monitors within and on the periphery of urban environments as meteorological conditions can influence NO_2

NAWAZ ET AL. 13 of 22



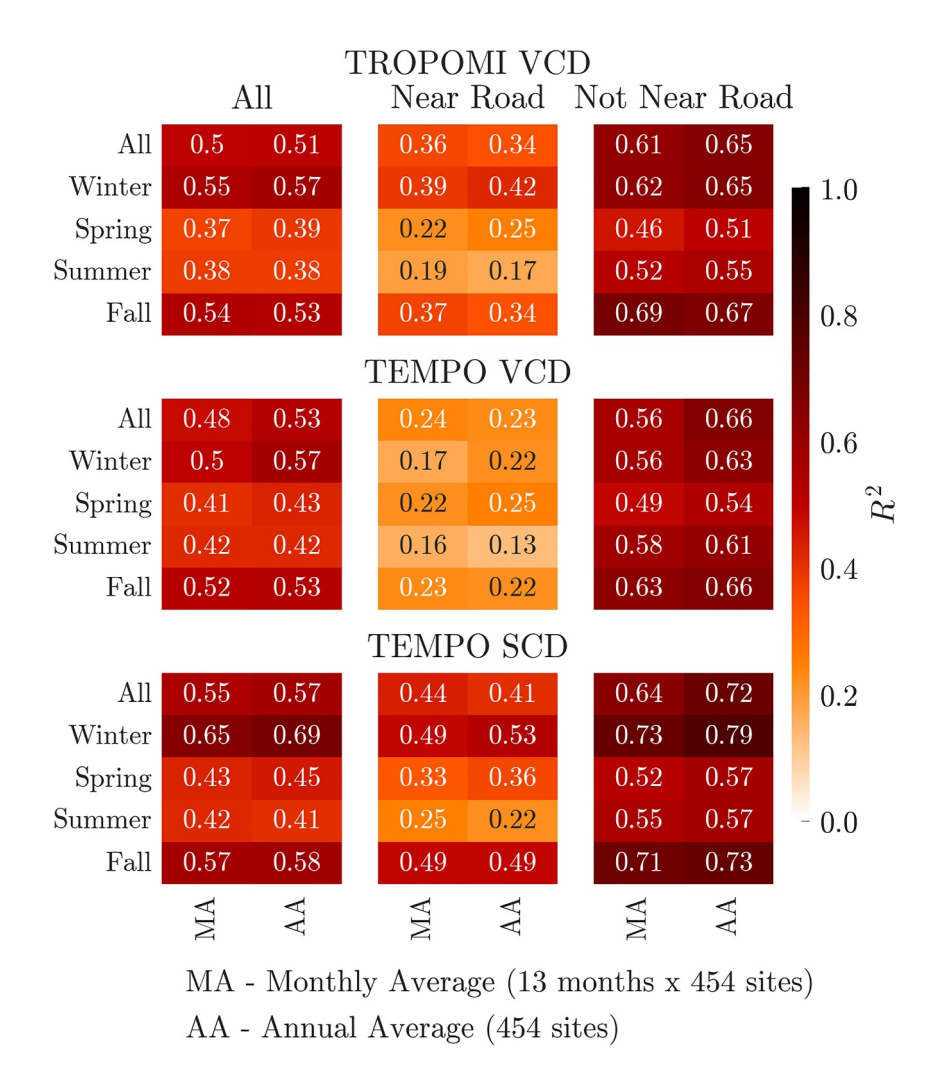


Figure 6. Correlation between AQS surface-level monitors and TROPOMI VCDs (top), TEMPO VCDs (middle), and TEMPO SCDs (bottom) for all monitors (left), near road monitors (middle), and not near road monitors (right).

differently dependent on proximity to sources within city centers. For the 222 monitors located within one of the urban boundaries (Figure 7a), correlation is generally strongest for hours when BLH below 839m, where it ranges from $R^2 = 0.27$ to $R^2 = 0.31$. For higher BLH, correlation steadily degrades down to $R^2 = 0.12$. This degradation in correlation is accompanied by reduced range: whereas the range is highest for AQS for low BLHs before stabilizing above 737 m, the range in TEMPO data decreases as BLHs increase, which corresponds to the early morning when TEMPO is at its peak (Figure 1). For the 125 monitors located on the periphery of cities (i.e., not within the urban boundaries but within 50 km of the city center), correlation is more strongly influenced by BLH: correlation is highest below 627m ($R^2 = 0.41$ to $R^2 = 0.46$) and afterward continuously decreases down to $R^2 = 0.03$ for hr with the highest BLH decile. For these periphery sites, AQS NO₂ distributions decrease with higher BLH; however, TEMPO column NO₂ distributions (i.e., boxplots) are generally unaffected except for higher BLHs (1,135 m and greater), although dynamic ranges consistently decrease with higher BLHs.

Ultimately, these results suggest that TEMPO column observations are generally better correlated with surface NO_2 for periods during which there are shallower BLH; this is likely attributable to the fact that when BLHs are deeper, surface-level NO_2 can be vertically mixed upwards to higher altitudes and the column NO_2 values are less representative of what is happening at the surface. However, we note that the ERA5 data are spatially coarse—introducing uncertainty into our results—and thus, it would be beneficial for future studies to explore this relationship by considering locations with collocated BLH observations with monitors and TEMPO, such as with the Unified Ceilometer Network (https://ucn-portal.org/) or field campaign data collected from airborne lidars

NAWAZ ET AL. 14 of 22

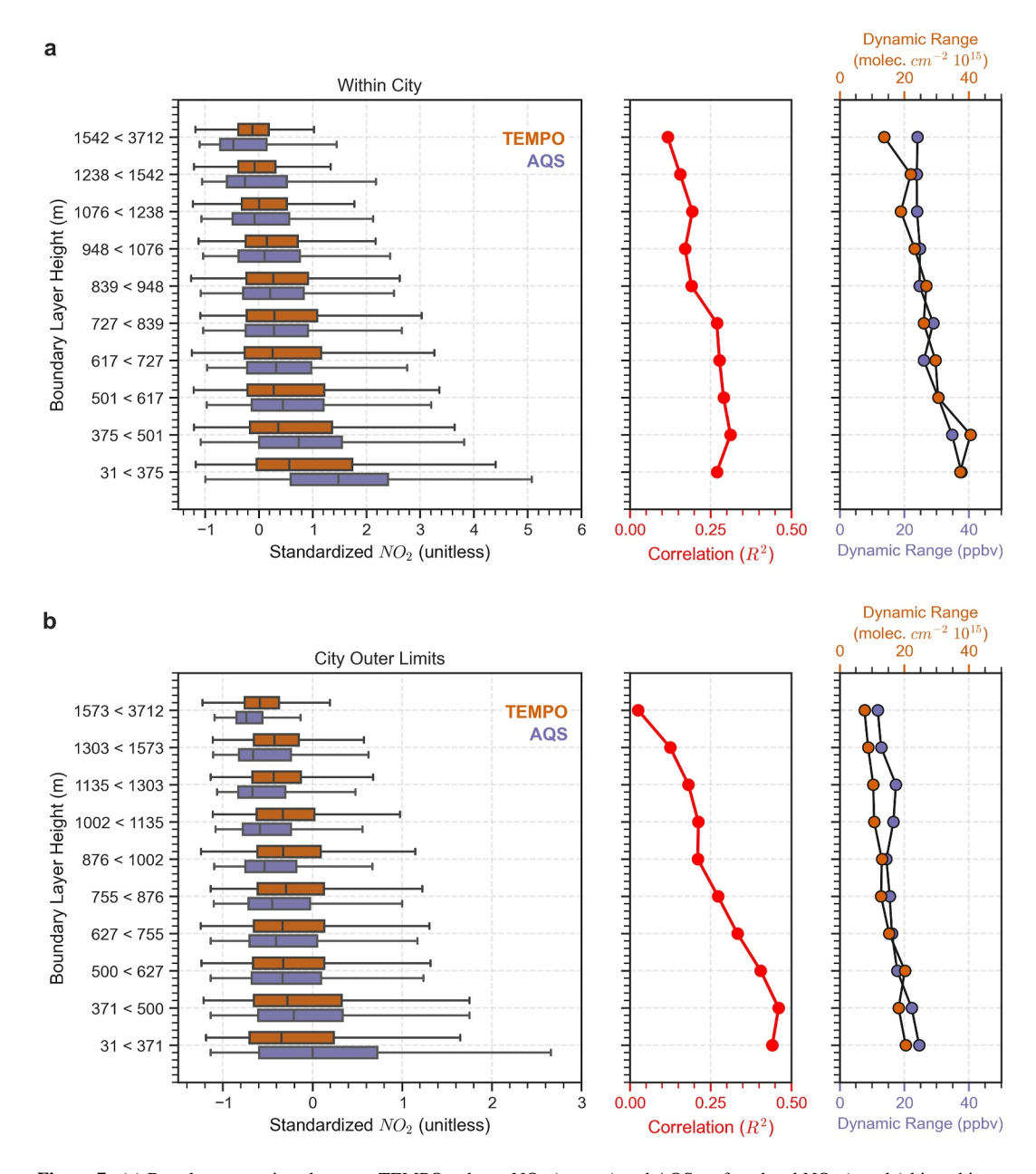


Figure 7. (a) Boxplot comparison between TEMPO column NO_2 (orange) and AQS surface-level NO_2 (purple) binned into equal size groups based on ERA5 boundary layer height for monitors located within one of the GHS-SMOD urban boundaries. The R^2 values and dynamic ranges for each bin are included in separate subplots to the right. (b) Same as but for monitors located on the periphery of cities, that is, monitors outside of urban boundaries but within 50 km of city centers.

(e.g., Scarino et al., 2014) such as those from the Synergistic TEMPO Air Quality Science mission (STAQS; https://www-air.larc.nasa.gov/missions/staqs/index.html). We additionally explore the relationship between column and surface NO₂ and BLHs across different seasons (Figure S14 in Supporting Information S1) and regions of the US (Figure S15 in Supporting Information S1). Although the trends identified across all data are generally consistent for individual seasons and regions, we note that in the Spring and Summer, the surface-level response to NO₂ at lower BLH values is suppressed and it is enhanced in cooler months with less active photochemistry. Regionally, the relationship between column and surface-level NO₂ and BLH is consistent.

We further explore the relationship between meteorology and NO₂ by considering monthly averaged hourly advection. We distinguish monitors within urban areas (Figure 8a) from those on the periphery of urban areas (Figure 8b)—that is, monitors not within urban boundaries but within 50 km of a city center. Within cities,

NAWAZ ET AL. 15 of 22

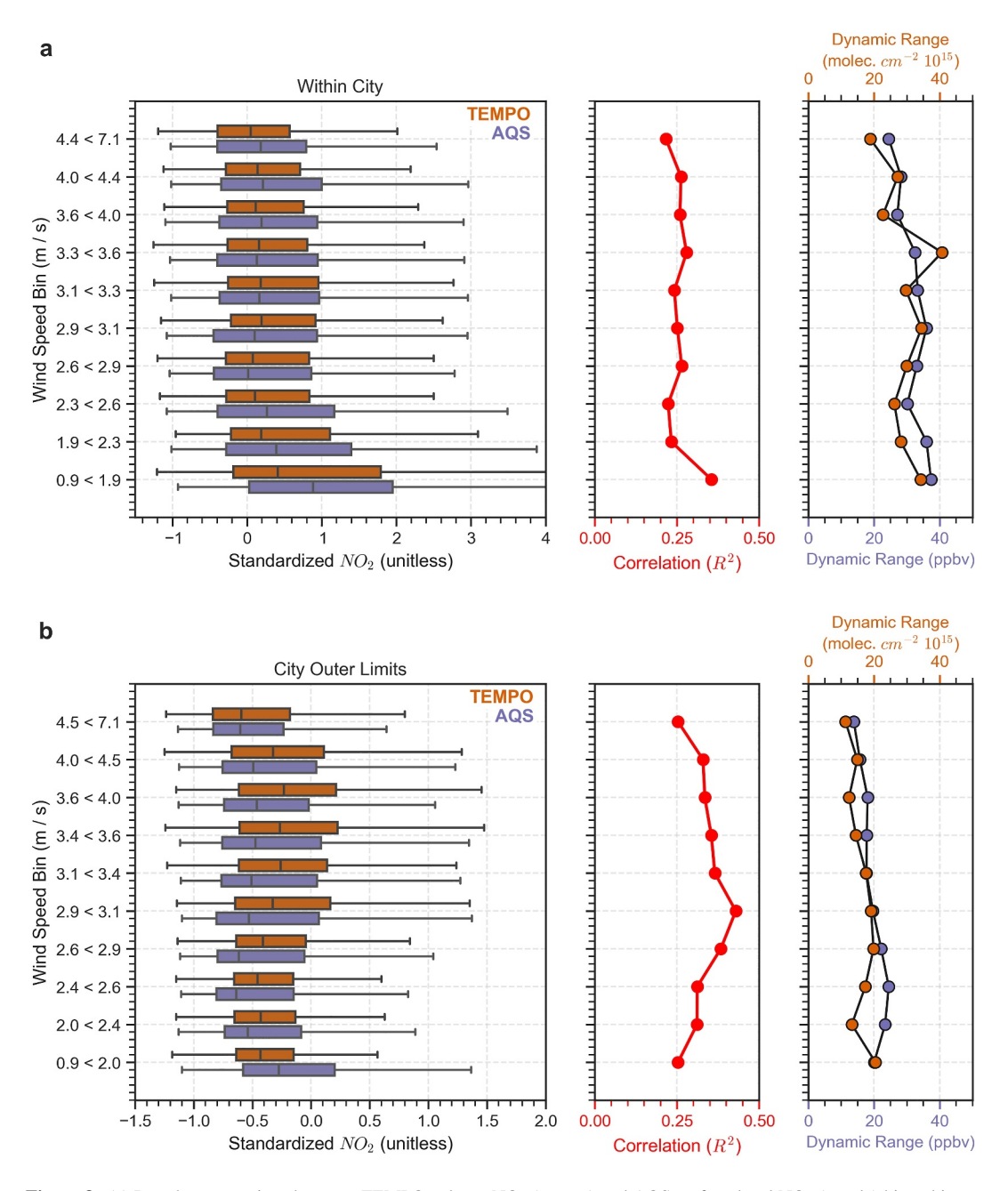


Figure 8. (a) Boxplot comparison between TEMPO column NO_2 (orange) and AQS surface-level NO_2 (purple) binned into deciles based on ERA5 wind speed for monitors located within a GHS SMOD urban boundary. R^2 and dynamic range values are included in separate plots to the right for the same wind bins. (b) Same as (a) but for monitors located outside of an urban boundary but within 50 km of a city center.

correlation is relatively stable across the less windy conditions above 1.9 m/s, R^2 ranges from 0.23 to 0.27; however, they are highest during low wind conditions of below 1.9 m/s with an $R^2=0.36$. This suggests that within these urban areas, correlations are poor (partially due to a higher number of near road monitors) and this could be attributable to heterogeneity in spatial distribution of NO_2 as the proximity to sources varies across different urban environments (Judd et al., 2018, 2019); however, correlations are strongest during stagnant conditions.

For monitors on the periphery of cities (Figure 8b), correlations peak at an intermediate wind speed of between 2.9 and 3.1 m/s ($R^2 = 0.45$); there is poorer correlation for periphery sites during low (between 0.9 and 1.9 m/s) and

NAWAZ ET AL. 16 of 22

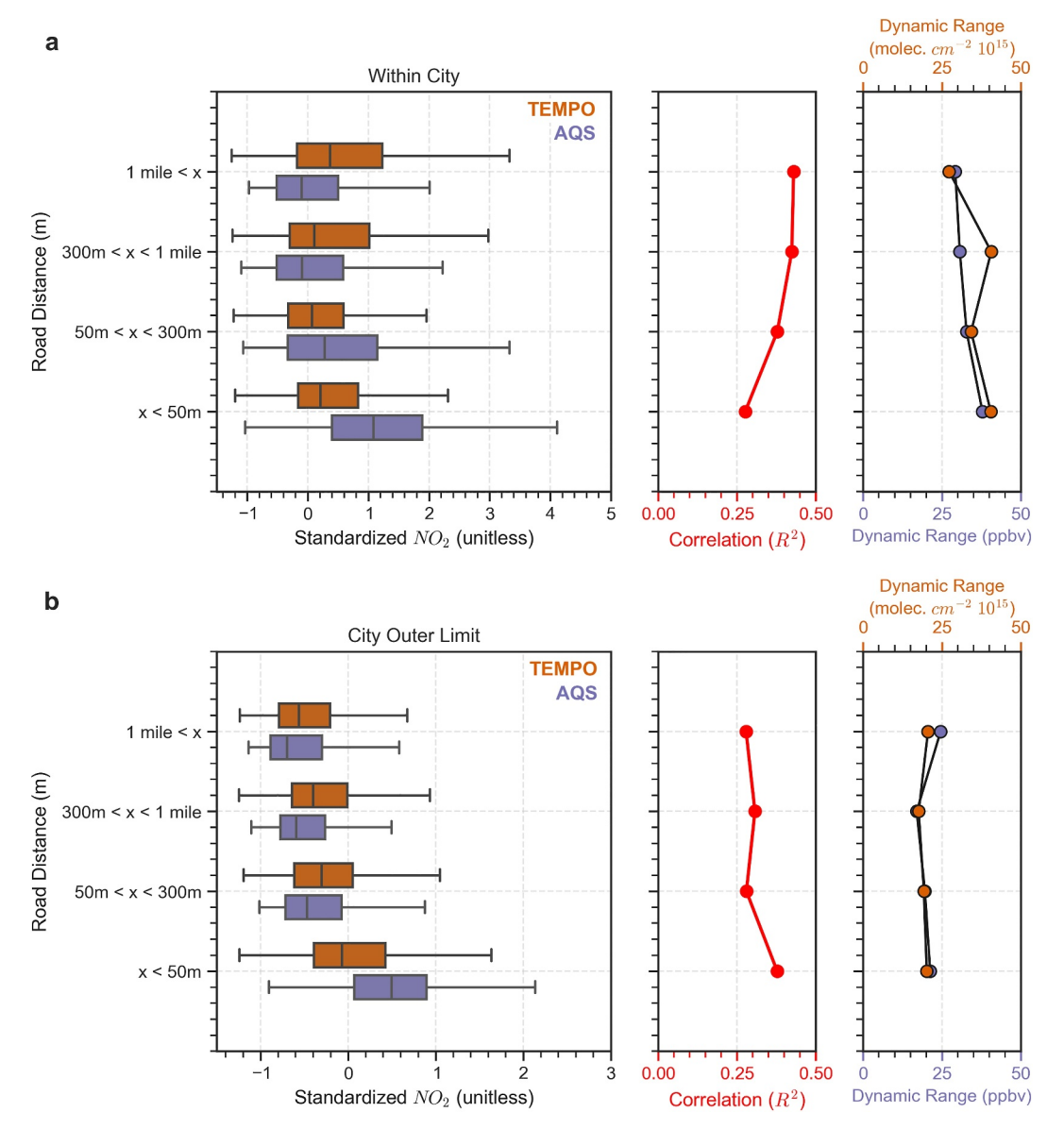


Figure 9. (a) Boxplot comparison between TEMPO column NO_2 (orange) and AQS surface-level NO_2 (purple) binned into four groups based on proximity to major roads derived from land-use data. R^2 and dynamic range values are included in separate plots to the right for the same wind bins. (b) Same as (a) but for monitors located outside of an urban boundary but within 50 km of a city center.

high (between 4.4 and 7.1 m/s) of $R^2 = 0.25$. Overall, despite there being fewer monitors of this type than urban sites, agreement is slightly better. This suggests that for monitors within the periphery of urban areas, higher wind speeds will likely have less of an effect on correlation than for other monitors.

Beyond meteorological conditions, the proximity of a monitor to major roadways has implications for both TEMPO and AQS correlation and concentrations. We bin TEMPO and AQS NO_2 observations based on their distance from the nearest major roadway (refer to Section 2.4 for details) to compare the two. We again distinguish monitors within urban areas (Figure 9a) from those on the periphery (Figure 9b). For the prior group, monitors that are directly adjacent to roads (<50 m) observe 1.8 times higher NO_2 than other monitors; however, TEMPO column NO_2 are only 1.1 times higher at these monitors. For this group of monitors that is closest to major roadways, correlation between surface-level and column NO_2 is the lowest ($R^2 = 0.28$). As monitors are located further from major roadways, correlations improve from $R^2 = 0.38$ (between 50 and 300 m), to $R^2 = 0.42$ (between 300m and 1 mile), and finally to $R^2 = 0.43$ (greater than 1 mile). Relatedly, both TEMPO column and

NAWAZ ET AL. 17 of 22



AQS surface-level NO_2 levels decrease as monitor distance from the nearest road increases. Within cities, column and surface-level NO_2 exhibit clear differences in behavior relative to major roadways; TEMPO column NO_2 is better correlated and more representative of surface-level observations for monitor locations that are greater than 1 mile from roadways.

The behavior of correlation—relative to road proximity—is flipped for monitors on the periphery of cities (Figure 9b). Correlations are highest for the monitors closest to roadways or $R^2 = 0.38$ (<50 m) and are similarly lower for other distances $R^2 = 0.28$ (between 50 and 300 m), $R^2 = 0.31$ (between 300 m and 1 mile), and $R^2 = 0.28$ (greater than 1 mile). For these city periphery monitors, the near road increase in average NO₂ is more notable than the within city sites. Those that are directly adjacent to roads (<50 m) observe 2.6 times higher NO₂ than other monitors; however, TEMPO column NO₂ are only 1.3 times higher at these sites. These results suggest that for these periphery sites, TEMPO agrees better with AQS monitors and observes elevated levels near major roads; however, given that they are on the edges of cities, this agreement may be due to a lesser variety of sources other than roads.

4. Discussion

TEMPO remote-sensing provides exciting enhancements to characterize tropospheric NO_2 ; however, there are specific seasonal, meteorological, and monitor characteristics that affect its correlation with surface-level NO_2 . Although column NO_2 observed from TEMPO often exhibits similar diurnal patterns to surface-level NO_2 in a general sense, there are weaker hour-to-hour decrease between 8:00 and 9:00 LT that are likely driven by differences in the two distinct measurements such as how responsive they are to BLH dynamics. This suggests that as the boundary-layer height increases in the morning, there are sharper changes in NO_2 levels observed at the surface than what is observed in the column. In the later afternoon and early evening, both TEMPO and the AQS observe slight increases in NO_2 levels at the near road monitors but decreases at those monitors that are not near road, which may be signals attributable to increased traffic NO_x ; however, this cannot be definitively determined without the implementation of source apportionment analyses.

Considering correlation, we find that TEMPO column and AQS surface-level NO_2 are especially well correlated at the not near road sites ($R^2 = 0.49$) compared to the near road sites ($R^2 = 0.22$). It is likely that the $2 \times 4.75 \text{ km}^2$ resolution of TEMPO—and the additional NO_2 captured at levels above the surface—limit the ability of current satellite derived remote sensing to capture the sharp gradients in NO_2 within 20 m of major road systems. This is a fundamental difference between the spatial representativeness of TEMPO and AQS observations; TEMPO observes the average column across grid cells whereas the AQS monitors observe concentrations at a specific point in space. Thus, throughout our analyses, differences between the two may be attributable to the distinct spatial representations that are captured in their sampling. Previous work has partially explored this through the comparison of surface-level monitoring with Pandora spectrometry. One study found that although Pandora and in situ NO_2 were generally well correlated, they could vary substantially by location and season (Knepp et al., 2015) and more recent studies have confirm this finding that although the relationship between Pandora column and in situ surface NO_2 are often fairly linear, they have distinct spatial and diurnal variability (Chang et al., 2022; Tao et al., 2025).

Across all monitors, TEMPO column and AQS surface-level NO₂ were most poorly correlated in the early morning (6:00–7:00 LT) and the strongest correlated in the mid to late morning (8:00–11:00 LT) before slowly decreasing throughout the day; however, this pattern did not occur in the wintertime in which correlations continued to rise throughout the morning and early afternoon peaking at 14:00 LT before decreasing sharply. In the early morning hours, uncertainty in the TEMPO retrievals may be higher as sensitivity of the instrument to near-surface pollution is degraded from a longer sunlight path through the atmosphere. Directly after this, the boundary layer height is still generally low compared to later in the day; this shallower boundary layer height is likely responsible for greater correlation between column and surface-level NO₂ as vertical mixing is more restricted during these hours. As the boundary layer height increases in the late morning and early afternoon, surface-level NO₂ is more vertically mixed, and correlations degrade. This is reflected in the dynamic ranges of TEMPO data in which ranges are highest in the early morning and lowest in the late afternoon; relatedly, some of the poorer correlation in the afternoon could be attributable to lower dynamic ranges.

Seasonally, column to surface correlations were lowest in the spring $(R^2 = 0.37)$ and summer $(R^2 = 0.38)$ and highest in winter $(R^2 = 0.41)$ and fall $(R^2 = 0.46)$. In the US, generally, there is more active photochemistry

NAWAZ ET AL. 18 of 22



associated with NO₂ in the spring and summer months and thus lower concentrations and a smaller dynamic range. Given these lower concentrations, NO₂ concentrations are closer to instrument noise levels during these periods that could weaken the correlations. In the winter months, when NO₂ levels are higher due to less active photochemistry, noise likely has less of an effect on correlation. Spatially, correlations are generally stronger in East Coast US states and weaker in states at higher latitudes, most notably, in the Midwest and Mountain West. For these high latitude states, monitors generally have smaller dynamic ranges that likely are partially responsible for these weaker correlations. We also find that SCDs outperform the VCDs throughout much of the day outside of the mid to late afternoon during which SCDs and VCDs are comparably correlated with surface-level NO₂. These results support prior findings that the AMF is the largest contributor to uncertainty in the algorithm (Lorente et al., 2017b); this previous work specifically implicate differences in the a priori trace gases, surface albedo, and cloud parameters as the greatest contributors to AMF uncertainty. Thus, locations and times of day with any cloud coverage could be especially sensitive to this uncertainty along with regions with high surface albedo including those with high snow coverage and urban environments.

Meteorological conditions affect column to surface correlation. TEMPO observations taken during shallowest BLHs are much stronger correlated ($R^2 = 0.27$) with the surface than those at the highest ($R^2 = 0.12$) for urban monitors but even to a greater extent for monitors on the periphery of cities ($R^2 = 0.44$ to $R^2 = 0.03$). When the BLH is shallower—and the column NO₂ is more closely aligned with surface-level NO₂—TEMPO may reveal more accurate information about what NO₂ looks like at the surface. Notably, surface-level NO₂ is much more responsive to BLH than column NO₂; in the bottom five deciles, as BLH decreases surface-level NO₂ increases, whereas column NO₂ remains relatively stable. Dynamic ranges for both the AQS and TEMPO are smallest in the deepest BLH conditions, thus this degradation in correlation associated with BLH could partially be associated with lower ranges. For monitors in the periphery of cities (outside of the urban extent but within 50 km of the city center), correlations were stronger during lower wind speeds (<1.4 m/s) and worsen for increased wind speeds. The proximity of monitors to road systems also affects correlation; for monitors in cities, TEMPO observations are better correlated with surface-level NO₂ taken at monitors furthest away from major roads ($R^2 = 0.43$) than at monitors within 20 m of major roads ($R^2 = 0.28$). This relationship does not hold for monitors on the periphery of cities. For these monitors, correlation is maximized near roads ($R^2 = 0.38$) and generally stable for other locations (ranges from $R^2 = 0.28$ to $R^2 = 0.31$).

There are many sources of uncertainty and assumptions that could affect our findings in comparing TEMPO column to AQS surface-level NO_2 . Our results are only representative for the current TEMPO vertical column density retrieval algorithm; as the algorithm is updated, the relationships between column NO_2 and surface-level NO_2 across different conditions will likely be affected and hopefully improved. Additionally, there is a well-documented high bias in chemiluminescent NO_2 monitors that we do not correct for; if there are areas in which reactive nitrogen species are higher or lower—relative to NO_2 —this could affect the overall correlations. All of our analysis is conducted using monthly averaged NO_2 to reduce variability and for more relevance to the longer-term data that is relevant for health exposures; however, we note that there is a great degree of daily variability in the data that is removed through this averaging. This is especially possible for meteorological conditions (i.e., the BLH and wind speeds) or transient burning events that are averaged out that have a high degree of daily variability that is not captured in monthly averages. Thus, our findings should not be extended to consider relationships between column and surface-level NO_2 at daily timescales and should only be considered for monthly, seasonal, or annual timescales. Lastly, the meteorological data that we use from ERA5 are spatially coarse $(0.25^{\circ} \times 0.25^{\circ})$. Thus, they do not capture finer-scale variability in meteorological conditions, such as sea breezes, that would have implications for comparisons between TEMPO column and AQS surface-level NO_2 .

With these uncertainties in mind, this work has implications for applications of TEMPO data. Generally, TEMPO matches the diurnal patterns of surface-level NO₂ between the late morning and early afternoon; however, our results suggest that patterns differ at the edges of the day when TEMPO data are more dependent on a priori information due to a longer sunlight path through the atmosphere. Given this, we suggest that V03 TEMPO NO₂ data should only be applied to infer surface-level concentrations during the late morning to early afternoon period 8:00 to 14:00 LT. Additionally, we find that for particular seasons and spatiotemporal averages, TEMPO struggles to capture fine-scale NO₂ gradients near major roads. Currently, SCDs are better correlated with surface-level NO₂ than VCDs; thus, through the SCD and VCD comparisons conducted in this work, uncertainty introduced by the AMF could be better quantified and in turn, the VCDs may improve in the future. This could benefit applications for estimating surface NO₂ as generally the VCDs are most interpretable. In the interim,

NAWAZ ET AL. 19 of 22



SCDs could be used as a predictor variable for surface level estimates. This could benefit applications for estimating surface NO_2 as generally the VCDs are included as a predictor variable for surface level estimates. There are still outstanding questions such as how well the patterns in monthly averaged NO_2 , characterized in this study, carry over to finer temporal resolution (i.e., daily) and how well the results found for this study period (August 2023-August 2024) would hold for other years or multiyear averages. Ultimately, our analysis characterizes the conditions and characteristics under which TEMPO column NO_2 agrees with surface-level NO_2 . These characterizations have implications for future efforts to infer surface-level estimates of NO_2 through the application of deterministic, statistical, or machine-learning approaches, which are crucial in identifying the health effects associated with NO_2 pollution.

Conflict of Interest

The authors declare no conflicts of interest relevant to this study.

Data Availability Statement

All TEMPO NO₂ data are available from NASA EARTHDATA Atmospheric Science Data Center as the TEMPO_NO2_L2_V03 product (NASA/LARC/SD/ASDC, n.d.). Pregenerated US EPA AQS data are publicly available (U.S. Environmental Protection Agency, 2025). ERA5 data are available from the Copernicus Climate Data Store (Copernicus Climate Change Service, 2023). Road proximity data are from (Acker et al., 2025).

Acknowledgments References

We gratefully acknowledge the computing resources provided on the high performance computing cluster operated by Research Technology Services at the George Washington University.

Additionally, we acknowledge funding from NASA Earth Science Division grants 80NSSC23K1002, 80NSSC21K0511, 80NSSC21K0427, and 80NSSC24K0503.

- Achakulwisut, P., Brauer, M., Hystad, P., & Anenberg, S. C. (2019). Global, national, and urban burdens of paediatric asthma incidence attributable to ambient NO₂ pollution: Estimates from global datasets. *The Lancet Planetary Health*, 3(4), e166–e178. https://doi.org/10.1016/S2542-5196(19)30046-4
- Acker, S. J., Holloway, T., & Harkey, M. K. (2025). Satellite detection of NO₂ distributions and comparison with ground-based concentrations (pp. 1–39). EGUsphere. https://doi.org/10.5194/egusphere-2025-226
- Anenberg, S. C., Mohegh, A., Goldberg, D. L., Kerr, G. H., Brauer, M., Burkart, K., et al. (2022). Long-term trends in urban NO₂ concentrations and associated paediatric asthma incidence: Estimates from global datasets. *The Lancet Planetary Health*, 6(1), e49–e58. https://doi.org/10.1016/S2542-5196(21)00255-2
- Appel, K. W., Napelenok, S. L., Foley, K. M., Pye, H. O. T., Hogrefe, C., Luecken, D. J., et al. (2017). Description and evaluation of the Community Multiscale Air Quality (CMAQ) modeling system version 5.1. Geoscientific Model Development, 10(4), 1703–1732. https://doi. org/10.5194/gmd-10-1703-2017
- Chang, L.-S., Kim, D., Hong, H., Kim, D.-R., Yu, J.-A., Lee, K., et al. (2022). Evaluation of correlated Pandora column NO₂ and in situ surface NO₂ measurements during GMAP campaign. *Atmospheric Chemistry and Physics*, 22(16), 10703–10720. https://doi.org/10.5194/acp-22-10703-2022
- Chen, X., Qi, L., Li, S., & Duan, X. (2024). Long-term NO2 exposure and mortality: A comprehensive meta-analysis. *Environmental Pollution*, 341, 122971. https://doi.org/10.1016/j.envpol.2023.122971
- Choi, S., Lamsal, L. N., Follette-Cook, M., Joiner, J., Krotkov, N. A., Swartz, W. H., et al. (2020). Assessment of NO₂ observations during DISCOVER-AQ and KORUS-AQ field campaigns. Atmospheric Measurement Techniques, 13,2523–2546. https://doi.org/10.5194/amt-13-2523-2020
- Cooper, M. J., Martin, R. V., McLinden, C. A., & Brook, J. R. (2020). Inferring ground-level nitrogen dioxide concentrations at fine spatial resolution applied to the TROPOMI satellite instrument. *Environmental Research Letters*, 15(10), 104013. https://doi.org/10.1088/1748-9326/aba3a5
- Copernicus Climate Change Service. (2023). ERA5 hourly data on single levels from 1940 to present [Dataset]. https://doi.org/10.24381/cds.
- Cordioli, M., Pironi, C., De Munari, E., Marmiroli, N., Lauriola, P., & Ranzi, A. (2017). Combining land use regression models and fixed site monitoring to reconstruct spatiotemporal variability of NO₂ concentrations over a wide geographical area. *Science of the Total Environment*, 574, 1075–1084. https://doi.org/10.1016/j.scitotenv.2016.09.089
- Courrèges-Lacoste, G. B., Sallusti, M., Bulsa, G., Bagnasco, G., Veihelmann, B., Riedl, S., et al. (2017). The Copernicus Sentinel 4 mission: A geostationary imaging UVN spectrometer for air quality monitoring. In Sensors, Systems, and Next-Generation Satellites XXI (Vol. 10423, pp. 62–70). https://doi.org/10.1117/12.2282158
- Dickerson, R. R., Anderson, D. C., & Ren, X. (2019). On the use of data from commercial NOx analyzers for air pollution studies. *Atmospheric Environment*, 214, 116873. https://doi.org/10.1016/j.atmosenv.2019.116873
- European Commission. (2025). Retrieved from https://human-settlement.emergency.copernicus.eu/ghs_smod2023.php
- Flynn, C. M., Pickering, K. E., Crawford, J. H., Lamsal, L., Krotkov, N., Herman, J., et al. (2014). Relationship between column-density and surface mixing ratio: Statistical analysis of O₃ and NO₂ data from the July 2011 Maryland DISCOVER-AQ mission. *Atmospheric Environment*, 92, 429–441. https://doi.org/10.1016/j.atmosenv.2014.04.041
- GBD 2021 Risk Factor Collaborators. (2024). Global burden and strength of evidence for 88 risk factors in 204 countries and 811 subnational locations, 1990–2021: A systematic analysis for the global burden of disease study 2021. *The Lancet*, 403(10440), 2162–2203. Retrieved from https://www.thelancet.com/journals/lancet/article/PIIS0140-6736(24)00933-4/fulltext
- Geddes, J. A., Martin, R. V., Bucsela, E. J., McLinden, C. A., & Cunningham, D. J. M. (2018). Stratosphere–troposphere separation of nitrogen dioxide columns from the TEMPO geostationary satellite instrument. Atmospheric Measurement Techniques, 11(11), 6271–6287. https://doi.org/10.5194/amt-11-6271-2018

NAWAZ ET AL. 20 of 22



- GeoPandas Development Team. (2025). GeoPandas. (1.0.1) [Computer software]. Open Source Geospatial Foundation. Retrieved from https://
- Glissenaar, I., Boersma, K. F., Anglou, I., Rijsdijk, P., Verhoelst, T., Compernolle, S., et al. (2025). TROPOMI level 3 tropospheric NO₂ Dataset with Advanced Uncertainty Analysis from the ESA CCI+ ECV Precursor Project. Earth System Science Data Discussions, 1–36. https://doi.org/10.5194/essd-2024-616
- Goldberg, D. L., Anenberg, S. C., Kerr, G. H., Mohegh, A., Lu, Z., & Streets, D. G. (2021). TROPOMI NO2 in the United States: A detailed look at the annual averages, weekly cycles, effects of temperature, and correlation with surface NO₂ concentrations. *Earth's Future*, 9(4), e2020EF001665. https://doi.org/10.1029/2020EF001665
- González Abad, G., Nowlan, C. R., Wang, H., Chong, H., Houck, J., Liu, X., & Chance, K. (2024b). *Tropospheric Emissions: Monitoring of Pollution (TEMPO) project trace gas and cloud level 2 and 3 data products: User guide (user's guide no. version 1.2)*. Havrard & Smithsonian. Retrieved from https://asdc.larc.nasa.gov/documents/tempo/guide/TEMPO_Level-2-3_trace_gas_clouds_user_guide_V1.2.pdf
- González Abad, G., Liu, X., Chance, K., Wang, H., Kurosu, T. P., & Suleiman, R. (2015). Updated Smithsonian Astrophysical Observatory Ozone Monitoring Instrument (SAO OMI) formaldehyde retrieval. Atmospheric Measurement Techniques, 8(1), 19–32. https://doi.org/10.5194/amt-8-19-2015
- González Abad, G., Nowlan, C. R., Wang, H., Chong, H., Houck, J., Liu, X., & Chance, K. (2024a). TEMPO trace gas and cloud level 2 and 3 data products: User guide. Retrieved from https://asdc.larc.nasa.gov/documents/tempo/guide/TEMPO_Level-2-3_trace_gas_clouds_user_guide_V1.2.pdf
- Harkey, M., & Holloway, T. (2024). Simulated surface-column NO₂ connections for satellite applications. *Journal of Geophysical Research:*Atmospheres, 129(21), e2024JD041912, https://doi.org/10.1029/2024JD041912
- Hersbach, H., Bell, B., Berrisford, P., Hirahara, S., Horányi, A., Muñoz-Sabater, J., et al. (2020). The ERA5 global reanalysis. *Quarterly Journal of the Royal Meteorological Society*, 146(730), 1999–2049. https://doi.org/10.1002/qj.3803
- Jacob, D. J., Heikes, E. G., Fan, S.-M., Logan, J. A., Mauzerall, D. L., Bradshaw, J. D., et al. (1996). Origin of ozone and NOx in the tropical troposphere: A photochemical analysis of aircraft observations over the South Atlantic basin. *Journal of Geophysical Research*, 101(D19), 24235–24250. https://doi.org/10.1029/96JD00336
- Judd, L. M., Al-Saadi, J. A., Janz, S. J., Kowalewski, M. G., Pierce, R. B., Szykman, J. J., et al. (2019). Evaluating the impact of spatial resolution on tropospheric NO₂ column comparisons within urban areas using high-resolution airborne data. Atmospheric Measurement Techniques, 12(11), 6091–6111. https://doi.org/10.5194/amt-12-6091-2019
- Judd, L. M., Al-Saadi, J. A., Valin, L. C., Pierce, R. B., Yang, K., Janz, S. J., et al. (2018). The dawn of geostationary air quality monitoring: Case studies from Seoul and Los Angeles. Frontiers in Environmental Science, 6, 85. https://doi.org/10.3389/fenvs.2018.00085
- Keller, C. A., Knowland, K. E., Duncan, B. N., Liu, J., Anderson, D. C., Das, S., et al. (2021). Description of the NASA GEOS composition forecast modeling system GEOS-CF v1.0. *Journal of Advances in Modeling Earth Systems*, 13(4), e2020MS002413. https://doi.org/10.1029/ 2020MS002413
- Khreis, H., Kelly, C., Tate, J., Parslow, R., Lucas, K., & Nieuwenhuijsen, M. (2017). Exposure to traffic-related air pollution and risk of development of childhood asthma: A systematic review and meta-analysis. *Environment International*, 100, 1–31. https://doi.org/10.1016/j. envint.2016.11.012
- Kimbrough, S., Chris Owen, R., Snyder, M., & Richmond-Bryant, J. (2017). NO to NO₂ conversion rate analysis and implications for dispersion model chemistry methods using Las Vegas, Nevada near-road field measurements. *Atmospheric Environment*, 165, 23–34. https://doi.org/10. 1016/j.atmoseny.2017.06.027
- Knepp, T., Pippin, M., Crawford, J., Chen, G., Szykman, J., Long, R., et al. (2015). Estimating surface NO₂ and SO₂ mixing ratios from fast-response total column observations and potential application to geostationary missions. *Journal of Atmospheric Chemistry*, 72(3), 261–286. https://doi.org/10.1007/s10874-013-9257-6
- Lamsal, L. N., Krotkov, N. A., Celarier, E. A., Swartz, W. H., Pickering, K. E., Bucsela, E. J., et al. (2014). Evaluation of OMI operational standard NO₂ column retrievals using in situ and surface-based NO₂ observations. Atmospheric Chemistry and Physics, 14(21), 11587–11609. https://doi.org/10.5194/acp-14-11587-2014
- Lamsal, L. N., Martin, R. V., van Donkelaar, A., Steinbacher, M., Celarier, E. A., Bucsela, E., et al. (2008). Ground-level nitrogen dioxide concentrations inferred from the satellite-borne Ozone Monitoring Instrument. *Journal of Geophysical Research*, 113(D16). https://doi.org/10.
- Larkin, A., Anenberg, S., Goldberg, D. L., Mohegh, A., Brauer, M., & Hystad, P. (2023). A global spatial-temporal land use regression model for nitrogen dioxide air pollution. Frontiers in Environmental Science, 11, 1125979. https://doi.org/10.3389/fenvs.2023.1125979
- Laughner, J. L., & Cohen, R. C. (2019). Direct observation of changing NOx lifetime in North American cities. *Science*, 366(6466), 723–727. https://doi.org/10.1126/science.aax6832
- Lee, H. J., Kim, N. R., & Shin, M. Y. (2024). Capabilities of satellite Geostationary Environment Monitoring Spectrometer (GEMS) NO2 data for hourly ambient NO2 exposure modeling. *Environmental Research*, 261, 119633. https://doi.org/10.1016/j.envres.2024.119633
- Lerdau, M. T., Munger, J. W., & Jacob, D. J. (2000). The NO₂ flux conundrum. Science, 289(5488), 2291–2293. https://doi.org/10.1126/science. 289.5488.2291
- Levelt, P. F., Joiner, J., Tamminen, J., Veefkind, J. P., Bhartia, P. K., Stein Zweers, D. C., et al. (2018). The ozone monitoring instrument: Overview of 14 years in space. *Atmospheric Chemistry and Physics*, 18(8), 5699–5745. https://doi.org/10.5194/acp-18-5699-2018
- Li, Y., Xing, C., Peng, H., Song, Y., Zhang, C., Xue, J., et al. (2023). Long-term observations of NO₂ using GEMS in China: Validations and regional transport. Science of the Total Environment, 904, 166762. https://doi.org/10.1016/j.scitotenv.2023.166762
- Lindsey, D. T., Heidinger, A. K., Sullivan, P. C., McCorkel, J., Schmit, T. J., Tomlinson, M., et al. (2024). GeoXO: NOAA's future geostationary satellite system. *Bulletin of the American Meteorological Society*, 105(3), E660–E679. https://doi.org/10.1175/BAMS-D-23-0048.1
- Lorente, A., Folkert Boersma, K., Yu, H., Dörner, S., Hilboll, A., Richter, A., et al. (2017a). Structural uncertainty in air mass factor calculation for NO₂ and HCHO satellite retrievals. *Atmospheric Measurement Techniques*, 10(3), 759–782. https://doi.org/10.5194/amt-10-759-2017
- Lorente, A., Folkert Boersma, K., Yu, H., Dörner, S., Hilboll, A., Richter, A., et al. (2017b). Structural uncertainty in air mass factor calculation for NO₂ and HCHO satellite retrievals. *Atmospheric Measurement Techniques*, 10(3), 759–782. https://doi.org/10.5194/amt-10-759-2017
- NASA/LARC/SD/ASDC. (n.d.). TEMPO NO₂ tropospheric and stratospheric columns V03 (PROVISIONAL) [Dataset]. NASA Langley Atmospheric Science Data Center DAAC. Retrieved from https://doi.org/10.5067/IS-40e/TEMPO/NO2_L2.003
- Nawaz, M. O., Goldberg, D. L., Kerr, G. H., & Anenberg, S. C. (2025). TROPOMI satellite data reshape NO₂ air pollution land-use regression modeling capabilities in the United States. ACS ES&T Air, 2(2), 187–200. https://doi.org/10.1021/acsestair.4c00153
- Nawaz, M. O., Johnson, J., Yarwood, G., de Foy, B., Judd, L., & Goldberg, D. L. (2024). An intercomparison of satellite, airborne, and ground-level observations with WRF–CAMx simulations of NO₂ columns over Houston, Texas, during the September 2021 TRACER-AQ campaign. Atmospheric Chemistry and Physics, 24(11), 6719–6741. https://doi.org/10.5194/acp-24-6719-2024

NAWAZ ET AL. 21 of 22



- Nowlan, C. R., Abad, G. G., Liu, X., Wang, H., & Chance, K. (2025). TEMPO nitrogen dioxide retrieval algorithm theoretical basis document. Palmer, P. I., Jacob, D. J., Chance, K., Martin, R. V., Spurr, R. J. D., Kurosu, T. P., et al. (2001). Air mass factor formulation for spectroscopic measurements from satellites: Application to formaldehyde retrievals from the global ozone monitoring experiment. *Journal of Geophysical Research*, 106(D13), 14539–14550. https://doi.org/10.1029/2000JD900772
- Penn, E., & Holloway, T. (2020). Evaluating current satellite capability to observe diurnal change in nitrogen oxides in preparation for geo-stationary satellite missions. *Environmental Research Letters*, 15(3), 034038. https://doi.org/10.1088/1748-9326/ab6b36
- Richmond-Bryant, J., Snyder, M. G., Owen, R. C., & Kimbrough, S. (2018). Factors associated with NO₂ and NOX concentration gradients near a highway. *Atmospheric Environment*, 174, 214–226. https://doi.org/10.1016/j.atmosenv.2017.11.026
- Scarino, A. J., Obland, M. D., Fast, J. D., Burton, S. P., Ferrare, R. A., Hostetler, C. A., et al. (2014). Comparison of mixed layer heights from airborne high spectral resolution lidar, ground-based measurements, and the WRF-Chem model during CalNex and CARES. Atmospheric Chemistry and Physics, 14(11), 5547–5560. https://doi.org/10.5194/acp-14-5547-2014
- Tao, M., Fiore, A. M., Karambelas, A., Miller, P. J., Valin, L. C., Judd, L. M., et al. (2025). Insights into summertime surface ozone formation from diurnal variations in formaldehyde and nitrogen dioxide along a transect through New York City. *Journal of Geophysical Research: Atmospheres*, 130(9), e2024JD040922. https://doi.org/10.1029/2024JD040922
- U.S. Environmental Protection Agency. (2025). Air quality system data mart [Dataset]. Retrieved from https://www.epa.gov/outdoor-air-quality-data
- US EPA, O. (2014). NAAQS table [other policies and guidance]. Retrieved from https://www.epa.gov/criteria-air-pollutants/naaqs-table
- US EPA, O. (2020). Near road monitoring [data and tools]. Retrieved from https://www.epa.gov/amtic/near-road-monitoring
- Veefkind, J. P., Aben, I., McMullan, K., Förster, H., de Vries, J., Otter, G., et al. (2012). TROPOMI on the ESA Sentinel-5 precursor: A GMES mission for global observations of the atmospheric composition for climate, air quality and ozone layer applications. Remote Sensing of Environment, 120, 70–83. https://doi.org/10.1016/j.rse.2011.09.027
- WHO. (2025). WHO. Retrieved from https://www.who.int/health-topics/air-pollution
- Yang, L. H., Jacob, D. J., Dang, R., Oak, Y. J., Lin, H., Kim, J., et al. (2024a). Interpreting Geostationary Environment Monitoring Spectrometer (GEMS) geostationary satellite observations of the diurnal variation in nitrogen dioxide (NO₂) over East Asia. Atmospheric Chemistry and Physics, 24(12), 7027–7039. https://doi.org/10.5194/acp-24-7027-2024
- Yang, L. H., Jacob, D. J., Dang, R., Oak, Y. J., Lin, H., Kim, J., et al. (2024b). Interpreting Geostationary Environment Monitoring Spectrometer (GEMS) geostationary satellite observations of the diurnal variation in nitrogen dioxide (NO₂) over East Asia. Atmospheric Chemistry and Physics, 24(12), 7027–7039. https://doi.org/10.5194/acp-24-7027-2024
- Zhang, R., Tie, X., & Bond, D. W. (2003). Impacts of anthropogenic and natural NOx sources over the U.S. on tropospheric chemistry. *Proceedings of the National Academy of Sciences*, 100(4), 1505–1509. https://doi.org/10.1073/pnas.252763799
- Zoogman, P., Liu, X., Suleiman, R. M., Pennington, W. F., Flittner, D. E., Al-Saadi, J. A., et al. (2017). Tropospheric emissions: Monitoring of pollution (TEMPO). *Journal of Quantitative Spectroscopy and Radiative Transfer*, 186, 17–39. https://doi.org/10.1016/j.jqsrt.2016.05.008

NAWAZ ET AL. 22 of 22